University of Windsor
Scholarship at UWindsor

Electronic Theses and Dissertations | Theses, Dissertations, and Major Papers

2005

The localization of protein disulfide isomerase and further evidence towards its role as a neuroprotective protein in SH-SY5Y cells.

Dana Seslija
University of Windsor

Follow this and additional works at: https://scholar.uwindsor.ca/etd

Recommended Citation

Seslija, Dana, "The localization of protein disulfide isomerase and further evidence towards its role as a neuroprotective protein in SH-SY5Y cells." (2005). *Electronic Theses and Dissertations*. 4087.
https://scholar.uwindsor.ca/etd/4087

This online database contains the full-text of PhD dissertations and Masters' theses of University of Windsor students from 1954 forward. These documents are made available for personal study and research purposes only, in accordance with the Canadian Copyright Act and the Creative Commons license—CC BY-NC-ND (Attribution, Non-Commercial, No Derivative Works). Under this license, works must always be attributed to the copyright holder (original author), cannot be used for any commercial purposes, and may not be altered. Any other use would require the permission of the copyright holder. Students may inquire about withdrawing their dissertation and/or thesis from this database. For additional inquiries, please contact the repository administrator via email (scholarship@uwindsor.ca) or by telephone at 519-253-3000ext. 3208.

NOTE TO USERS

This reproduction is the best copy available.

UMI®

Reproduced with permission of the copyright owner. Further reproduction prohibited without permission.

Reproduced with permission of the copyright owner. Further reproduction prohibited without permission.

The Localization of Protein Disulfide Isomerase and Further Evidence Towards its Role as a Neuroprotective Protein in SH-SY5Y Cells

by

Dana Seslija

A Thesis

Submitted to the Faculty of Graduate Studies

and Research

through the Department of Chemistry and Biochemistry

in Partial Fulfillment of the Requirements for

the Degree of Master of Science at the

University of Windsor

Windsor, Ontario, Canada

2005

©2005 D. Seslija

Reproduced with permission of the copyright owner. Further reproduction prohibited without permission.

Library and Archives Canada

Published Heritage Branch

395 Wellington Street
Ottawa ON K1A 0N4
Canada

Bibliothèque et Archives Canada

Direction du Patrimoine de l'édition

395, rue Wellington
Ottawa ON K1A 0N4
Canada

Your file Votre référence
ISBN: 0-494-09801-5
Our file Notre référence
ISBN: 0-494-09801-5

NOTICE:
The author has granted a non-exclusive license allowing Library and Archives Canada to reproduce, publish, archive, preserve, conserve, communicate to the public by telecommunication or on the Internet, loan, distribute and sell theses worldwide, for commercial or non-commercial purposes, in microform, paper, electronic and/or any other formats.

The author retains copyright ownership and moral rights in this thesis. Neither the thesis nor substantial extracts from it may be printed or otherwise reproduced without the author's permission.

AVIS:
L'auteur a accordé une licence non exclusive permettant à la Bibliothèque et Archives Canada de reproduire, publier, archiver, sauvegarder, conserver, transmettre au public par télécommunication ou par l'Internet, prêter, distribuer et vendre des thèses partout dans le monde, à des fins commerciales ou autres, sur support microforme, papier, électronique et/ou autres formats.

L'auteur conserve la propriété du droit d'auteur et des droits moraux qui protège cette thèse. Ni la thèse ni des extraits substantiels de celle-ci ne doivent être imprimés ou autrement reproduits sans son autorisation.

In compliance with the Canadian Privacy Act some supporting forms may have been removed from this thesis.

While these forms may be included in the document page count, their removal does not represent any loss of content from the thesis.

Conformément à la loi canadienne sur la protection de la vie privée, quelques formulaires secondaires ont été enlevés de cette thèse.

Bien que ces formulaires aient inclus dans la pagination, il n'y aura aucun contenu manquant.

Canada

Reproduced with permission of the copyright owner. Further reproduction prohibited without permission.

1027222

Abstract

Protein disulfide isomerase (PDI) is a multifunctional protein most well characterized for its ability to form and exchange disulfide bonds (Darby *et al.*, 1996). More recently, a host of other functions have been added to the resumé of this protein, including denitrosation activity (Zai *et al.*, 1999), mediation of integrin-dependent adhesion (Lahav *et al.*, 2000), and copper binding activity (Narindrasorasak *et al.*, 2003). PDI is a 110 kDa homodimer and contains five domains, *a-b-b'-a'c* (Darby *et al.*, 1996). The *a* and *a'* domains contain the Cys-Gly-His-Cys active site residues responsible for the thiol-disulfide exchange reactions (Darby *et al.*, 1996). Although this protein is predominantly localized within the endoplasmic reticulum depending on the cell type, PDI has also been found in secretory vesicles, the Golgi, and the plasma membrane (Akagi *et al.*, 1988) of eukaryotic cells. In glial astrocytes, PDI is also found throughout the cytosol (Safran and Leonard, 1991), but its interaction between the cytoplasm and endoplasmic reticulum is not fully understood. Under ischemic stress, PDI is upregulated in rat forebrain cells, suggesting protection against cellular stresses (Tanaka *et al.*, 1999). The localization of PDI in differentiated human neuroblastoma SH-SY5Y cells was probed by the development of a recombinant fusion protein between green fluorescent protein GFP and PDI. SH-SY5Y cells expressing the recombinant reporter protein were also exposed to oxidative and ischemic stress, and examined for characteristics of apoptosis. These cells demonstrated that PDI provides a significant decrease in apoptotic traits as compared to the control cells. It was observed that there was reduced nuclear condensation, and maintainence of mitochondrial membrane potential. Cells containing the recombinant protein also showed an increased number of viable cells when exposed to hypoxic stress. These results suggest that PDI plays a role in the protective mechanism towards cellular stress. Excessive neuronal loss induced by oxidative stress is often seen in patients due to aging, strokes, and neurodegenerative diseases. The results obtained by using this cell line for the study of neuronal cell death have potential implication for strokes and human neurodegenerative diseases.

Reproduced with permission of the copyright owner. Further reproduction prohibited without permission.

for my father and mother

Reproduced with permission of the copyright owner. Further reproduction prohibited without permission.

Acknowledgements

I am deeply indebted to my supervisor, Dr. L. Lee for giving me the opportunity to further my studies in biochemistry. I am also grateful to the professors and members of all the second floor biochemistry lab groups for their guidance and support.

Reproduced with permission of the copyright owner. Further reproduction prohibited without permission.

Contents

Reproduced with permission of the copyright owner. Further reproduction prohibited without permission.

Reproduced with permission of the copyright owner. Further reproduction prohibited without permission.

Reproduced with permission of the copyright owner. Further reproduction prohibited without permission.

Reproduced with permission of the copyright owner. Further reproduction prohibited without permission.

List of Figures

Reproduced with permission of the copyright owner. Further reproduction prohibited without permission.

Reproduced with permission of the copyright owner. Further reproduction prohibited without permission.

List of Tables

Reproduced with permission of the copyright owner. Further reproduction prohibited without permission.

List of Abbrieviations

AD - *Alzheimer's Disease*

AIF - *Apoptosis Initiating Factor*

ATP - *Adenosine Triphosphate*

BDNF - *Brain Derived Neurotropic Factor*

BPTI - *Bovine Pancreatic Trypsin Inhibitor*

BSA - *Bovine Serum Albumin*

CATH - *Class(C), Architecture(A), Topology(T) and Homologous superfamily (H)*

CJD - *Creutzfeldt-Jakob Disease*

CMV IE - *Cytomegalovirus Immediate Early*

CoQ_{10} - *Coenzyme* Q_{10}

csPDI - *Cell Surface PDI*

DCFDA - *Dichloroflourescein Diacetate*

DNA - *2'-Deoxyribonucleic Acid*

Dsb - *Disulfide Bond*

DTNB - *5,5'-Dithio-Bis-3-Nitrobenzoate*

DTT - *Dithiothreitol*

EDTA - *Ethylenediaminetetraacetic acid*

ER - *Endoplasmic Reticulum*

FADD - *Fas-associated Death Domain*

GFP - *Green Fluorescent Protein*

GSH - *Glutathione (reduced)*

GSSG - *Glutathione (oxidized)*

GSNO - *S-Nitrosoglutathione*

Reproduced with permission of the copyright owner. Further reproduction prohibited without permission.

HUVEC - *Human Umbilical Vein Endothelial Cells*

MAPK - *Mitogen Activated Protein Kinase*

MTP - *Microsomal Triglyceride Transfer Protein*

MW - *Molecular Weight*

NADPH - *Nicotinamide Adenine Dinucleotide Phosphate*

NAT - *Napthotriazole*

NMR - *Nuclear Magnetic Resonance*

NO - *Nitric Oxide*

OD - *Optical Density*

PBS - *Phosphate Buffered Saline*

PCD - *Programmed Cell Death*

PDI - *Protein Disulfide Isomerase*

PTP - *Permeability Transition Pore*

ROS - *Reactive Oxygen Species*

RSNO - *S-Nitrosothiol*

SCOP - *Structural Classification of Proteins*

SDS-PAGE - *Sodium Dodecyl Sulphate Polyacrylamide Gel Electrophoresis*

TBS - *Tris-Buffered Saline*

TNF - *Tumor Necrosis Factor*

TRX - *Thioredoxin*

Reproduced with permission of the copyright owner. Further reproduction prohibited without permission.

Chapter 1

General Introduction

1.1 Protein Disulfide Isomerase

There are a multitude of events that occur in the endoplasmic reticulum (ER) of the cell such as lipid biosynthesis, calcium storage, and most notably protein synthesis and modification. The ER is composed of a system of membranes that extends throughout the cytosol, and connects to the nuclear envelope. Within this dynamic network, lies a powerhouse of a protein, and with every new experiment another title is added to its host of newly discovered functions and activities. Protein disulfide isomerase (PDI), is most widely known for its role in protein folding and disulfide bond isomerization. Before PDI was classified, early work on the protein described an enzyme able to catalyze thiol exchange reactions in protein folding (Goldberger *et al.*, 1964). Folding *in vitro* can take minutes to hours for disulfide formation to take place. In the 1964 paper by Goldberger and colleagues, the "microsomal protein" had a specific activity 88 times that of the"microsome" alone. There is a high concentration of PDI found in the ER - approximately 0.2 mM (Lyles and Gilbert, 1991). Also, PDI has a low affinity interacting with its substrates. This lack of substrate specificity would be consistent with its ability to isomerize disulfide bonds in a myriad of different proteins.

Reproduced with permission of the copyright owner. Further reproduction prohibited without permission.

1.1.1 PDI Structure

Mammalian PDI is approximately 57 000 Da, and is made of approximately 491 amino acid residues (Darby and Creighton, 1998). The length of the protein can be debatable depending on the inclusion of a leader peptide signal. Throughout this thesis, the human PDI sequence obtained from the cDNA from pET-11a will be used (Appendix A). This sequence matches the human PDI sequence patented by Kato and coworkers in 1991, with the removal of the beginning 20 amino acid signal sequence. Structural analysis of the 120 residue a domain (Kemmink, *et al.*, 1996), and 110 residue b domain (Kemmink, *et al.*, 1999) of human PDI places it in the thioredoxin superfamily (SCOP 52833, CATH 3.40.30.10)(Murzin *et al.*, 1995, Pearl *et al.*, 2005). An NMR structure of the full length protein has not yet been elucidated. The characteristic sequence Cys-Gly-His-Cys found in the active site domains of the protein bear high sequence and structural homology to another redox protein, thioredoxin, which is found in both prokaryotic and eukaryotic cells. The members of this superfamily share the vicinal thiols, but differ in the two amino acids found between, which can directly affect the catalytic activity of the protein (see section 1.1.2 Thioredoxin). The structure of mammalian PDI has been classified into five different domains; *a, b, b', a,* and *c* (figure 1.1) (Kemmink *et al.*, 1996). Although PDI is found predominantly in the ER, PDI has been identified as subunits of other proteins including prolyl-4-hydroxylase, an enzyme involved in post-translational hydroxylation of peptidyl proline residues, and microsomal triglyceride transfer protein complex (MTP), a protein that transports triglyceride and cholesterol esters across membranes (Wetterau *et al.*, 1991). PDI has been found to have sequence homology with other proteins of unrelated function. For example, the b domain contains sequence homology to calsequesterin, a protein which pools calcium in the sarcoplasmic reticulum of muscle cells (Noiva, 1999). Located in the c-domain are acidic residues thought to bind calcium, which suggests that PDI has calcium storage and buffering capacity (Corbett *et al.*, 1999).

Reproduced with permission of the copyright owner. Further reproduction prohibited without permission.

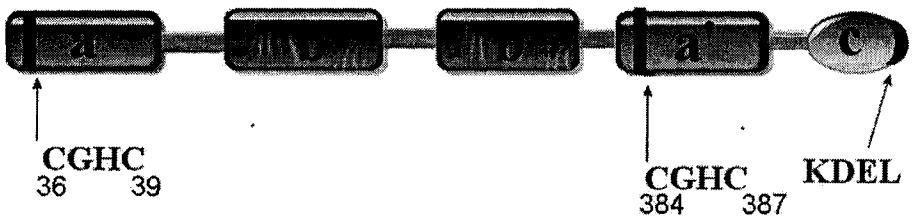

Figure 1.1: The structural domains of mammalian PDI. Kemmink and coworkers (1996) proposed this model of the structural domains of PDI. The location of the active site cysteines are found in the a and a' domains. The b and b' domains are responsible for chaperonic activity, and the c domain contains the carboxyl-terminal KDEL ER retention signal. The residue numbering is consistent with the sequence found in Appendix A.

Reproduced with permission of the copyright owner. Further reproduction prohibited without permission.

The activities of isolated a and a'domains are capable of catalyzing disulfide bond isomerization, but are less efficient than the entire PDI protein (Darby and Creighton, 1995), giving further proof for the importance of the other domains in the protein. The b' domain of PDI can bind unstructured regions of polypeptide to assist in the folding process (Freedman *et al.*, 2002). The importance of the b' domain to the chaperonic activity of PDI was demonstrated in a 2004 paper by Horibe and coworkers. By replacing the b domain in human protein disulfide isomerase related protein (hPDIR) with the b' domain from human PDI, the chaperonic activity of the protein was found to increase. The c domain has also been shown to help stabilize the chaperone function of the protein (Tian *et al.*, 2004). Also contained in the c domain is the KDEL sequence which is characteristic of controlling ER retention. Figure 1.2 shows the NMR structures of the a (left) and b (right) domains of PDI. Notice the two active site cysteines depicted in ball and stick imagery.

Reproduced with permission of the copyright owner. Further reproduction prohibited without permission.

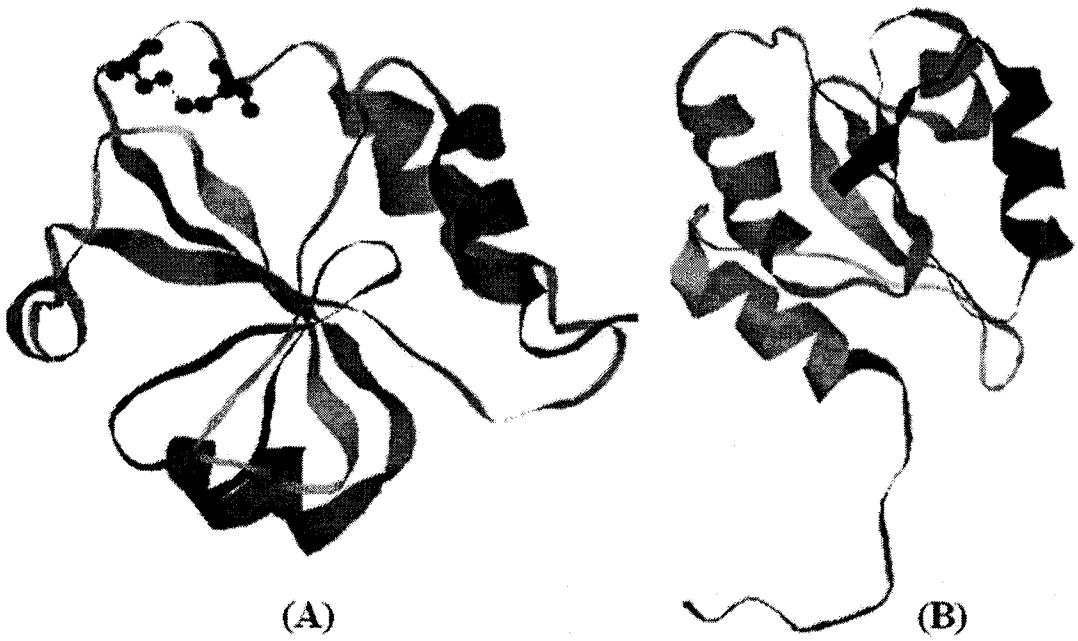

Figure 1.2: Domains a and b of human PDI from www.pdb.org (Berman *et al.*, 2000) (Date accessed 04/05/05). Figure (A) shows only one of 40 NMR structures of isolated human PDI a (A) domain. The active site cysteines are shown in ball and stick representation, located at residues 36 and 39. Figure (B) shows only one of 24 NMR structures of human PDI b (B) domain. Although not responsible for catalytic action, it is important for substrate stabilization. Accession number for the a domain is 1MEK, and b domain is 2BJX. The interactive Rasmol display was saved for each file, and structure modelling was done in Rasmol v.2.7.2.1.1.

Reproduced with permission of the copyright owner. Further reproduction prohibited without permission.

1.1.2 Thioredoxin

The thioredoxin (TRX) superfamily (SCOP 52833, CATH 3.40.30.10) consists of a group of proteins responsible for disulfide bond formation. The bacterial proteins include the Dsb (disulfide bond) and thioredoxin proteins. The bacterial disulfide bond (Dsb) proteins share the vicinal Cys residues in their active site (Table 1.1). The catalytic efficiency of the proteins are directed by the amino acids found between the two cysteines (Raina and Missiakas, 1997). Mutagenesis of the His-38 residue of PDI to Pro, makes this tetrapeptide sequence identical to thioredoxin, but results in a decrease in PDI activity (Lu *et al.*, 1992). The active site in the a domain (PDIa) is located between beta sheet three and alpha helix four - as shown in figure 1.2. Both the a and a' domains are highly homologous to TRX protein of bacterial cells. A common feature shared with thioredoxin is the alpha/beta fold of the a domain with the structure of $\beta\alpha\beta\alpha\beta\beta\alpha$ (Freedman *et al.*, 2002). The most notable difference between these proteins is that TRX exists in the periplasm of bacterial cells and catalyzes reductive reactions suitable to the reducing environment of the cells, whereas PDI exists predominantly within the less reducing ER, catalyzing both oxidative and reductive reactions.

Reproduced with permission of the copyright owner. Further reproduction prohibited without permission.

DsbA	**C**	P	H	**C**	*E. coli*
DsbB	**C**	V	L	**C**	*E. coli*
DsbC	**C**	G	Y	**C**	*E. coli*
DsbD	**C**	V	A	**C**	*E. coli*
DsbE	**C**	P	T	**C**	*E. coli*
Thioredoxin	**C**	G	P	**C**	*E. coli*
PDI-a	**C**	G	H	**C**	*H. sapiens*

Table 1.1: Members of the Thioredoxin Superfamily. A comparison of the active sites of 5 *E. coli* Dsb proteins, thioredoxin, and human PDI (Raina and Missiakas, 1997).

Reproduced with permission of the copyright owner. Further reproduction prohibited without permission.

1.1.3 PDI Disulfide Bond Rearrangement

The enzymatic goal of PDI is to replace reactive disulfides of its substrate with less reactive ones. This is based on a trial and error process, in which three different types of reactions take place: isomerization, reduction, and oxidation. This begins with PDI forming a complex with the misfolded substrate, so that one of the disulfides is disrupted to create a free sulfhydryl in the substrate. From the intermediate formed, the reaction can proceed in three different directions (Gilbert, 1997). The enzyme can be displaced, and the same disulfide bond will re-form so that no rearrangement occurs. The second reaction that can occur involves an intermolecular reaction between another substrate disulfide with the substrate thiol, to form a newly folded protein. Lastly, the substrate can be reduced to the original disulfide and then oxidized to form a different disulfide. In the last process, the second cysteine in the active site of PDI acts like a timer in that it induces reduction of the substrate, if a complex does not rearrange within a certain time. In the pink pathway of figure 1.3, simple rearrangement of substrate disulfides takes place. In the blue pathway of figure 1.3, it was proposed that the second cysteine prevents PDI from becoming trapped, in which PDI could 'escape', and reduction follwed by reoxidation of the substrate disulfides take place in a more timely manner. In more recent studies, PDI has been found to be involved in other activities such as integrin-dependent adhesion (Lahav *et al.*, 2000), and denitrosation of S-nitrosothiols (Zai *et al.*, 1999).

Reproduced with permission of the copyright owner. Further reproduction prohibited without permission.

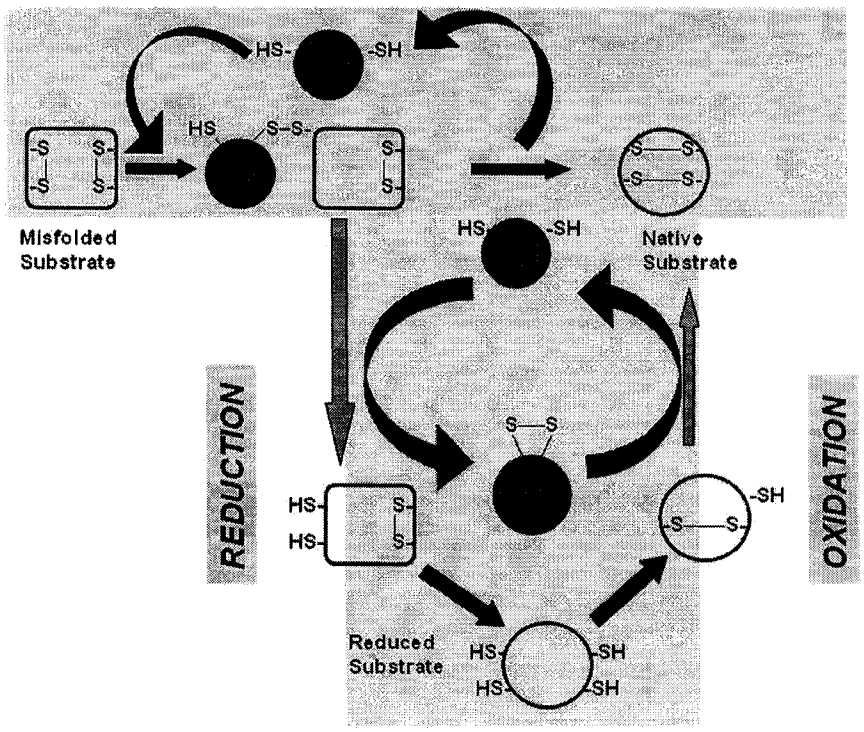

Figure 1.3: Disulfide rearrangement by PDI. A mechanism of disulfide rearrangement for PDI represents the different pathways that may occur during PDI- assisted protein folding (Schwaller *et al.*, 2003).

Reproduced with permission of the copyright owner. Further reproduction prohibited without permission.

1.1.4 Redox Control of PDI Activity

PDI is an oxidative enzyme performing its reactions in the less reducing ER (Raina and Missiakas, 1997), compared to the reducing environment of the cytoplasm. Thiol content determination in PDI is assessed by titration with 5,5'-dithio-*bis*-3-nitrobenzoate (DTNB). Freshly reduced bovine PDI was revealed to contain 1 free sulfhydryl and 3 disulfide bonds (Gilbert, 1989), although the exact location of these groups are not specified. The environment inside the endoplasmic reticulum has been found to favour thermodynamically the formation of disulfide bonds by increasing protein stability in the organelle. The conditions of this environment are created by the relative concentrations of glutathione in its reduced and oxidized form, GSH and GSSG. In the cytoplasm of cells the [GSH] to [GSSG] ratio is (30-100):1, whereas in the ER of cells, it is only 3:1 (Raina and Missiakas, 1997). This difference is important for PDI to stay in the predominantly reduced form, as its primary function is oxidation of proteins in disulfide bond formation. The active site of PDI contains a redox potential between -110 and -170 mV (Lundstrom and Holmgren, 1993). Outside of the ER, PDI is more likely to act as a reductant (Noiva, 1999).

1.1.5 Peptide Binding

PDI is able to act on a wide spectrum of substrates catalyzing thiol exchange reactions, and is largely dependent on its ability to bind to polypeptides. In this respect, PDI has a K_d less than 100 μM, indicating a low affinity for peptides (Morjana and Gilbert, 1991). In 1999, Koivunen and coworkers identified a peptide binding site in PDI, separate from the active site, between residues 452-461 in the a' domain. Studies involving mutation or deletion of the b, b', and c domain show evidence to support that these domains are involved in peptide binding. Mutation of the b' domain reduced isomerase activity (Darby and Creighton, 1998), and deletion of the c domain inhibited substrate binding activity (Dai and Wang, 1997). PDI exhibits increased affinity for polypeptides that contain a higher content of Cys residues (Klappa *et al.*, 1998), which correlates with its primary role in protein folding.

Reproduced with permission of the copyright owner. Further reproduction prohibited without permission.

1.1.6 Chaperone Activity

The true definition of a molecular chaperone is to "assist polypeptides to self-assemble by inhibiting alternative assembly pathways that produce non-functional structures" (*www.Biology-Online.com* 31/05/05). A well known molecular chaperone, GroEL/ES undergoes repeated cycles of folding and unfolding, until a more stable form of its substrate is attained (Todd *et al.*, 1996). In the same respect, PDI is thought to undergo a similar process in the formation and exchange of disulfide bonds in proteins (Walker and Gilbert, 1997). Generally chaperones work to inhibit the aggregation of substrate molecules. PDI does this by rapidly forming disulfide bonds in its substrate, and using its peptide binding sites to help prevent aggregation (Quan *et al.*, 1995). Ironically, depending on the concentration of PDI with respect to the substrate, PDI can act as an anti-chaperone in facilitating aggregation (Puig *et al.*, 1994). For example, low concentrations of PDI (10 μM) added to a solution of unfolded and reduced lysozyme causes the formation of insoluble aggregates containing PDI and lysosyme, but when higher concentrations of PDI (100 μM) are added, aggregation ceases (Goldberg *et al.*, 1991). PDI makes up 1% of total cell protein, whose sheer concentration may also assist with the folding process by inhibiting aggregation of unfolded proteins.

1.1.7 Cell Surface PDI (csPDI)

PDI has shown to be very unique with respect to its functions in the cell. PDI has been found on the plasma membrane of platelets (Chen *et al.*, 1995). This change in location suggests alternative functions of PDI. In lieu of the traditional activities of this protein in the ER, it has been involved in mediating integrin-dependent adhesion (Lahav *et al.*, 2000) and aggregation (Essex and Li, 1998) in blood platelets. Platelet adhesion is important for blood coagulation, and this adhesion pathway is mediated by adhesion receptor integrins. It is thought that there is disulfide exhange or free sulfhydryl participation on the integrins. Lahav and coworkers (2000) found that by blocking PDI activity, integrin adhesion is inhibited. Recent studies have also shown

Reproduced with permission of the copyright owner. Further reproduction prohibited without permission.

that csPDI also plays a role in nitric oxide release from S-nitrosothiols (Root *et al.*, 2004), which is discussed in section 1.1.9.

1.1.8 PDI Kinetics

In 1989, Gilbert first proposed a mechanism for PDI catalyzed disulfide reduction. Since then, many studies examining the folding pathways of ribonuclease A (Shin *et al.*, 2002), creatine kinase (Zhao *et al.*, 2005), and alcohol dehydrogenase (Primm *et al.*, 1996) have attempted to delineate models of PDI activity. In the 1989 study by Gilbert, a hexapeptide (CYIQNC) and reduced glutathione (GSH) were used to probe the kinetic mechanism of PDI. In this study, he examined the PDI-dependent production of GSSG coupled with the oxidation of GSH by PDI, with glutathione reductase activity in the presence of excess NADPH. It was found that there were three separate phases of reduction of PDI disulfide bonds: slow (k=0.0019 min^{-1}), medium (k=0.025 min^{-1}), and fast (k=0.21 min^{-1}) (figure. 1.4). The proposed mechanism is dependent on GSH concentration; elevating the GSH concentration results in an increase of the reduction of PDI. Unfortunately, kinetic obstacles in early experimentation did not account for certain variables such as the auto-oxidation of GSH to GSSG, the non-enzymatic reaction between the two substrates, and the reduction of PDI by GSH. Taking these factors into account, a hybrid mechanism was proposed based on GSH concentration. More current models by Gilbert and colleagues propose an "escape" mechanism, in which disulfide isomerization involves cycles of reduction and reoxidation (Schwaller *et al.*, 2003) (figure 1.3). This mechanism also suggests that at increased concentrations of GSH, the rate of isomerization is decreased because of competition with protein substrate oxidation (Schwaller *et al.*, 2003). Although there are no proven enzyme models for PDI, because of the diverse array of substrates PDI can act upon, PDI may provide a number different options, depending on the substrate involved.

Reproduced with permission of the copyright owner. Further reproduction prohibited without permission.

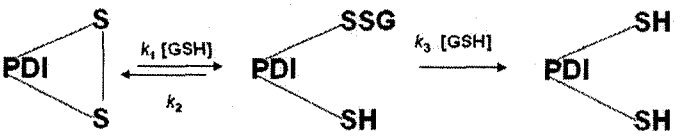

Figure 1.4: PDI catalyzed disulfide reduction. The initial mechanism was proposed in 1989 by Gilbert, but had not accounted for kinetic obstacles.

Reproduced with permission of the copyright owner. Further reproduction prohibited without permission.

1.1.9 Denitrosation Activity of PDI

Nitric oxide (NO) is most commonly known for its role in smooth muscle relaxation (Bernal-Mizrachi *et al.*, 2005), inhibition of platelet aggregation (Lincoln *et al.*, 1990), and molecular signalling (Linden *et al.*, 2005). S-nitrosothiols (RSNOs) are important transporters and donors of nitric oxides. Furthermore, RSNOs act as sinks for nitric oxide to prolong its half life, which varies inversely depending on its concentration in the cell. It has been shown that NO transfer from RSNOs is mediated by csPDI (Zai *et al.*, 1999). More recent work demonstrates the ability of PDI to store NO released from RSNOs, and denitrosate S-nitrosated PDI (PDI-SNO) at physiological pH (Sliskovic *et al.*, 2005). The proposed mechanism for PDI denitrosation begins with the transnitrosation of the a subunit with RSNO, and leads to the production of an unstable $NO^{\cdot}$ intermediate with an oxidized enzyme (figure. 1.5). Implications of this research demonstrate the importance of PDI in the movement of NO bound to RSNOs.

Reproduced with permission of the copyright owner. Further reproduction prohibited without permission.

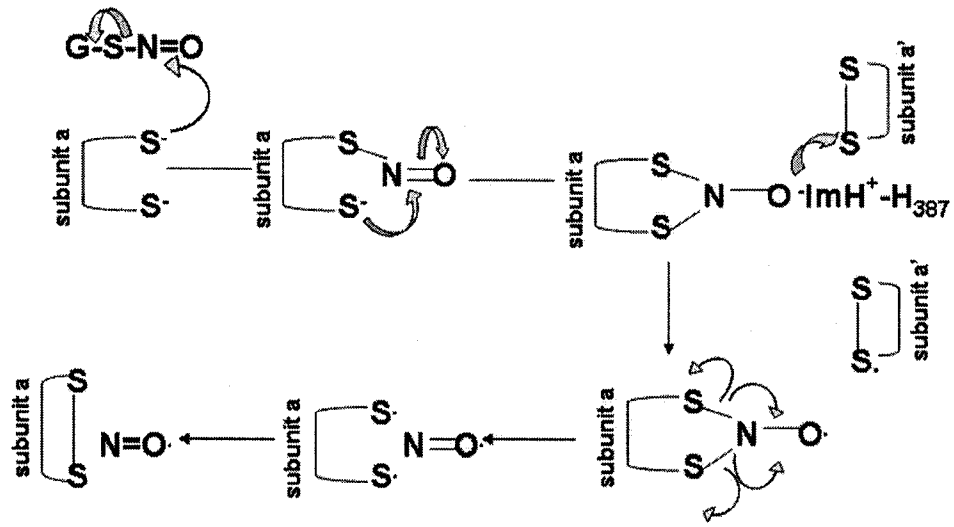

Figure 1.5: Mechanism for PDI denitrosation. Mutus and coworkers (2005), proposed a denitrosation mechanism with the active site of the a domain in PDI undergoing a transnitrosation reaction. The intermediate formed is shown to be stabilized by the imidazole group of His_{387} (numbers used are in accordance with the sequence found in appendix A). The final products are an oxidized protein, and $NO^{\cdot}$.

Reproduced with permission of the copyright owner. Further reproduction prohibited without permission.

1.2 Apoptosis

In all living organisms, every cell exists for a finite amount of time, before it dies. Cell death can be suicidal, but the death of a few cells may aid in maintaining tissue homeostasis. Alternatively, cell death can be uncontrollable by internal cell function, as it is imposed by outside variables such as physical damage, toxic chemicals, extreme heat or pressure. Each type of cell death has different features and markers by which they are characterized. Cell death by suicide is often referred to as programmed cell death (PCD), or apoptosis, whereas death by injury is referred to as necrosis. The term apoptosis was first coined in a 1972 paper by Kerr, Wyllie, and Currie with the pronounciation of a-poe-to-sis. Classical origins of this term orginate from Hippocrates (460-370 B.C.) in which he first used the word to describe bone erosion in relation to tissue death (*www.celldeath-apoptosis.org* 31/05/05).

1.2.1 Features of Necrosis Versus Apoptosis

Until the landmark study in 1972 by Kerr and colleagues, only necrotic cell death was studied. Damage to cells induced by trauma or damage causes cell swelling, membrane breakage, and release of lysosomal enzymes leading to inflammation damaging nearby cells (Gores *et al*, 1990). Conversely, apoptosis is stimulated by internal mechanisms within the cell and is a highly orchestrated process. Apoptosis occurs during development, in the immune system, in the inflammatory response, and in aging (Duke *et al.*, 1996). Death by suicide is characterized by cell shrinking and detachment, chromatin condensation, cytoplasmic membrane blebbing, the appearance of apoptotic bodies, and phagocytosis of the apoptotic bodies by macrophages (Kerr *et al.*, 1972) (figure. 1.6). Biochemical features include protein cleavage by caspases, and the expression of surface markers on apoptotic cells (Nagata, 2000). A prominent biochemical feature which distinguishes necrosis from apoptosis is the DNA fragmentation found in apoptosis, which is visualized as a ladder on an agarose gel. In necrosis, cell death can be almost instantaneous, in which the DNA remains undamaged, and this is indicated by a smear on an agarose gel.

Reproduced with permission of the copyright owner. Further reproduction prohibited without permission.

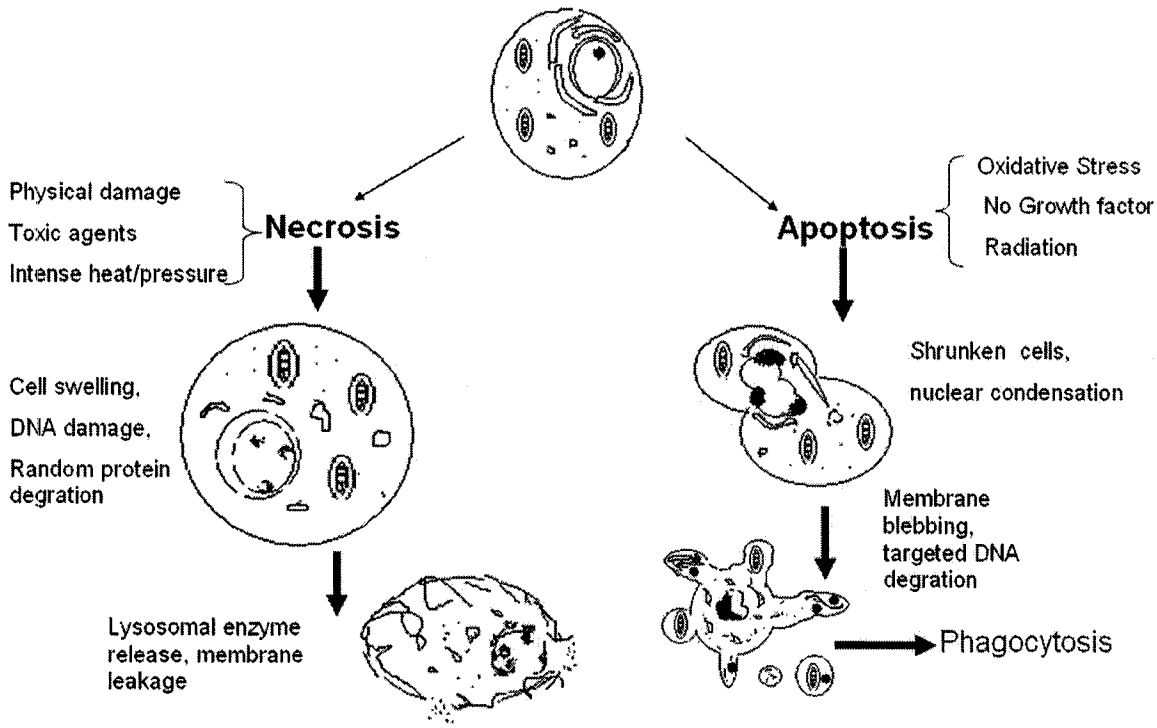

Figure 1.6: Necrosis vs. Apoptosis. The pathway to the left demonstrates cellular features of the necrotic pathway. The right side of the figure shows morphological features of apoptosis (Pollack and Leeuwenburgh, 2001).

Reproduced with permission of the copyright owner. Further reproduction prohibited without permission.

1.3 The Biochemical Mechanism of Apoptosis

Cell death can be initiated through four different mechanisms: receptor-mediated apoptosis, growth factor deprivation, oxidative stress, and genotoxic exposure. Once the pathway has begun, it can be divided into four different stages of progression (Hengartner, 2000). Apoptosis begins with a receptor or non-receptor mediated death signal, which signals the nucleus to initiate a suicide reponse. This is followed by a control and integration stage in which there is signal transduction, transcription factor activation, and ATP depletion. In the execution stage, cell death be carried out in two different pathways; a death receptor pathway (Ashkenazi and Dixit, 1998), or a mitochondrial pathway (Tatton and Olanow, 1999). Once these pathways have been initiated, the DNA degradation stage begins, and the cell begins to shrink and bleb, expressing phagocyte recognition molecules. In the final stage, phagocytosis occurs, removing dead cells and their debris (figure 1.6).

1.3.1 The Death Receptor Pathway

In the death receptor pathway, the binding of a ligand to a cell surface death receptor mediates a downstream death signal (Hengartner, 2000). These receptors belong to the tumor necrosis factor receptor (TNF) family. CD95 (also known as Fas or Apo1), a member of the TNF superfamily (SCOP 49599, CATH 2.60.210.10) (Murzin *et al.*, 1995, Pearl *et al.*, 2005), contains a characteristic cysteine-rich extracellular domain (Smith *et al.*, 1994), and a cytoplasmic "death domain" (Tartaglia *et al.*, 1993). Binding of a CD95 ligand (CD95L) to the CD95 receptor leads to the association of the death domains, and the binding of an adapter protein termed FADD (Fas-associated death domain) (figure 1.7). FADD contains a "death effector domain" which binds inactive caspase-8 (also known as FLICE or MACH). Once bound, the oligomerization of caspase-8 initiates self-cleavage, and activation of other caspases (Ashkenazi and Dixit, 1998). These caspases belong to a family of cysteine specific proteases (Thornberry and Yuri, 1998), which cleave peptide bonds at the carboxyl terminal side of aspartic acid residues (Villa *et al.*, 1997). There are many

Reproduced with permission of the copyright owner. Further reproduction prohibited without permission.

other receptors and pathways that have been shown to be involved in either initiating or protecting against apoptosis. The example of the CD95 mediated pathway has been shown to play a pivotal role in a different type of apoptosis (Nagata, 1997). These types include inflammatory cell death at "immune-privileged sites", virus or cancer-infected cell death by cytotoxic T and natural killer cells, and the deletion of activated mature T cells at the end of an immune response (Nagata, 1997).

Reproduced with permission of the copyright owner. Further reproduction prohibited without permission.

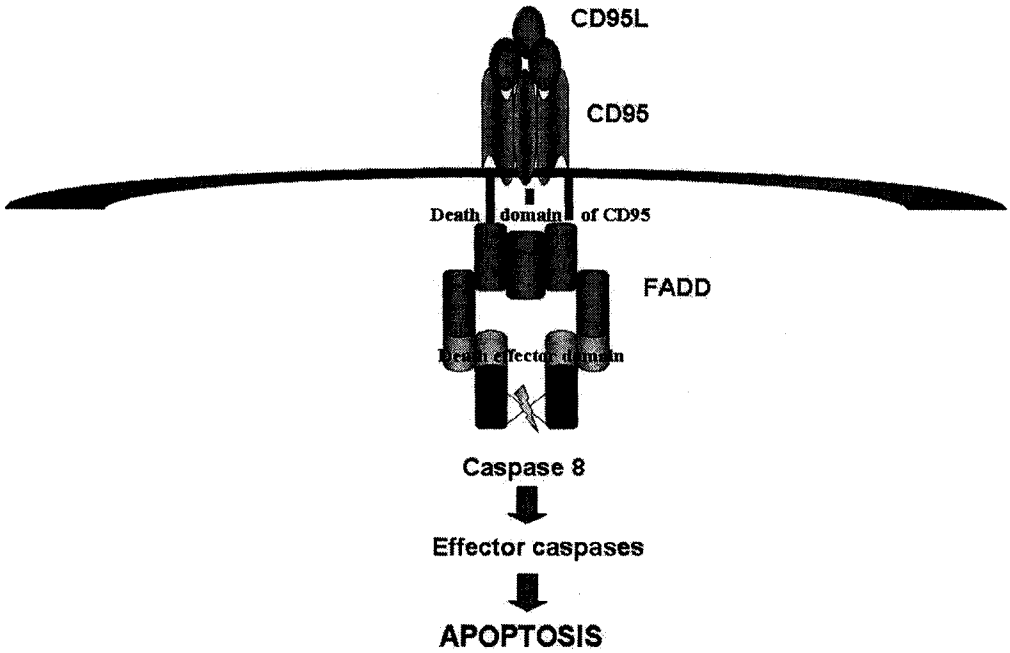

Figure 1.7: Apoptotic signalling through a death receptor pathway. Outside of the cell, CD95L binds to the CD95 trimeric receptor. Inside, adaptor protein FADD associates with the death domains of the CD95 receptor. Inactive caspase-8 then binds through the death effector domain of FADD, which initiates self-cleavage of caspase-8. This leads to the activation of other downstream caspases (Adapted from Ashkenazi and Dixit, 1998).

Reproduced with permission of the copyright owner. Further reproduction prohibited without permission.

1.3.2 The Mitochondrial Pathway

Mitochondria have been shown to play a very critical role in the apoptotic process. The disruption of the mitochondrial membrane potential ($\Delta\psi$) across the inner membrane causes the leakage of cytochrome c, apoptosis initiating factor (AIF), and caspase-9 into the cytoplasm (Kroemer *et al.*, 1997). These three factors together form an apoptosome, which leads to the activation of downstream caspases involved in the execution stage of apoptosis (figure 1.8). Although it is still not clear as to how they are released from the mitochondria, it is believed that following a decrease in mitochondrial membrane potential, a permeability transition pore (PTP) is opened in which cyt-c and other mitochondrial proteins are released (Tatton and Olanow, 1999). Mitochondria are the central location for oxidative phosphorylation, and the largest producer of reactive oxygen species (ROS) in the cell. Once disrupted, ROS are generated, and are highly reactive and cytotoxic to the cells (Betteridge, 2000). ROS has been have been shown to target mitochondrial DNA (Shoji *et al.*, 1995), mediate apoptosis (Kamata and Hirata, 1999), and even increase the prevalence of cancer in those individuals exposed to oxidative stress (Marnett, 2000).

Reproduced with permission of the copyright owner. Further reproduction prohibited without permission.

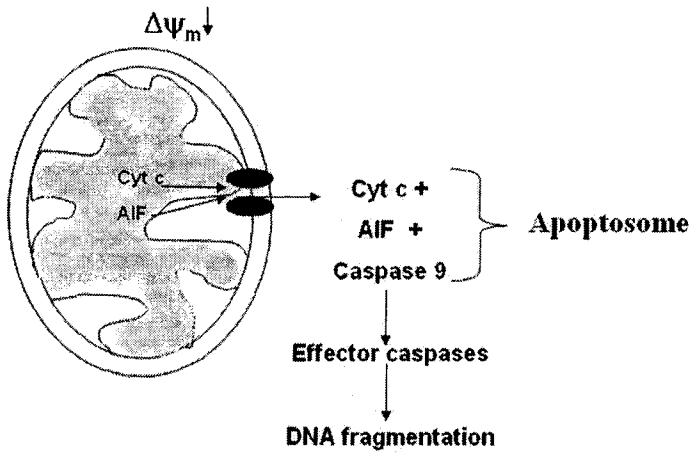

Figure 1.8: A hypothetical model of apoptotic initiation through the mitochondrial pathway. Following a decrease in mitochondrial membrane potential, a permeability transition pore (dark ovals) opens and cyt-c and AIF are released into the cytoplasm. By their associating with caspase-9, an apoptosome is formed, and downstream caspases are activated (Modified from Nomura, 2004).

Reproduced with permission of the copyright owner. Further reproduction prohibited without permission.

1.3.3 PDI as a Neuroprotective Protein

In a 2000 study, Tanaka and coworkers identified a stress protein up-regulated in response to hypoxia in glial cells. This protein was identified as PDI, and they found that its overexpression in primary cultured glial cells significantly reduced the loss of cell viability, when subjected to hypoxia. In the same study, Tanaka overexpressed PDI in different regions of rat brain and subjected them to ischemia. They observed that overexpression of PDI could suppress ischemia-induced apoptosis in the transfected area. PDI has been examined in conjunction with Alzheimer's disease (AD), which is characterized by the presence of neurofibrillary tangles, plaques, and degeneration of nerve cells (Corder *et al.*, 1993). During the development of Alzheimer's disease, it was noticed that during the shift in the redox balance of cells, there was no increase in PDI (Kim *et al.*, 2000). These scientists have postulated that the high levels of PDI that are found in neurons help to maintain the redox balance, but further oxidative damage may take place, because the concentration of the protein remains the same. Interestingly enough, PDI was found to be overexpressed in the brains of individuals with Creutzfeldt-Jakob disease (CJD) (Yoo *et al.*, 2002). More importantly, they were able to distinguish that PDI did not assist with the conformational change of the prion protein to a diseased form. Since the finding by Tanaka and coworkers in 2000, another protein that associates with PDI during cell death has been identified. Ubiquilin, which contains a ubiquitin-like domain and a ubiquitin-associated domain, are up-regulated during hypoxia in a similar time frame as PDI (Ko *et al.*, 2002). Furthermore, ubiquilin is up-regulated in neurons of AD patients in association with the neurofibrillary tangles (Mah *et al.*, 2000).

Apoptosis is a physiological requirement for the development and maintainence of tissue homeostasis. Disruption of this process, in which pathways become uncontrollable can result in diseases, in which there can be massive cell death, or no cell death at all. These include diseases such as Alzheimer's disease, Parkinson's disease, strokes, AIDS, auto-immune diseases, and cancers. In another example, PDI was characterized as a negative regulator of NF-κB, which is a transcription factor

Reproduced with permission of the copyright owner. Further reproduction prohibited without permission.

that induces an inflammatory response with acute and chronic immune and regeneration disorders (Higuchi *et al.*, 2004). It is important to continue to study PDI and understand completely the many ways in which this multifaceted protein functions.

Reproduced with permission of the copyright owner. Further reproduction prohibited without permission.

Chapter 2

Development, Expression, and Localization of PDI and its Active Site Domain

2.1 Objectives

Although PDI makes up approximately 1% of total protein content in cells (Goldberger *et al.*, 1964), an accessible source of human PDI is generally desirable for experimental studies and assays. Research to study the S-denitrosation activity of PDI (Sliskovic *et al.*, 2004), S-nitrosoglutathione consumption mediated by PDI (Root, *et al.*, 2004), and the development of more sensitive assays for the protein, required a readily attainable source of human PDI. To make this available, human PDI cDNA was cloned into the bacterial vector pET-28b containing two histidine tags (at the N-terminus and C-terminus) - see Appendix B. The vector was transformed into BL21(DE3) *E. coli* cells for simple purification of the recombinant protein through Ni^{2+} affinity chromatography. Also to isolate the source of activity in the protein for future study, the active site a domain was separately cloned into the pET-28b vector for further investigation on its copper binding abilities.

Characteristic of many ER resident proteins, PDI also contains the KDEL signal

Reproduced with permission of the copyright owner. Further reproduction prohibited without permission.

retention sequence. Although found predominantly in the ER, different isozymes of PDI have been identified in various cell types, which are not localized to the ER. To visualize the localization of PDI within neuroblastoma cells, human PDI cDNA was fused to green fluorescent protein in the pEGFP-N1 vector (Clontech), and transfected into SH-SY5Y cells. Differentiation of these cells further resolved its locale within this cell type. PDI, being a redox protein is readily influenced by its environment. Because PDI is well established as an ER protein, its localization outside of the ER is examined.

2.2 Materials and Methods

2.2.1 Chemicals, Biochemicals, and Supplies

- Bis-Acrylamide solutions were purchased from Bio-Rad Laboratories (Mississauga, ON).

- Restriction endonuclease EcoR1, *Taq* polymerase, direct load wide range DNA marker, direct load wide molecular weight range protein markers, low molecular weight range protein marker, ultra-low molecular weight range protein markers, high capacity nickel chelate affinity matrix (Ni-CAM HC RESIN), ampicillin, kanamycin, ribonuclease A (RNase), deoxyribonuclease I (DNase I), lysozyme, isopropylβ-D-thiogalactoside (IPTG), agarose, ammonium persulfate, brilliant blue R, calcium chloride, ethylenediaminetetraacetic acid (EDTA), glycine, imidazole, magnesium chloride hexahydrate, potassium acetate, potassium phosphate, sodium azide, phenylmethyl sulfonyl fluoride (PMSF), sodium chloride, trizma base, urea, tryptone, thiamine, tricine, zinc chloride, guanidine hydrochloride, protease inhibitor cocktail and 3',3',5',5'-tetramethylbenzidine were purchased from Sigma Aldrich (Oakville, ON).

- Restriction endonucleases *HindIII, PstI, KpnI, XhoI*, and T4 DNA Ligase were purchased from Promega Corporation (Madison, WI).

Reproduced with permission of the copyright owner. Further reproduction prohibited without permission.

- *Taq* Polymerase was kindly donated by Dr. S. Ananvoranich.
- Oligonucleotides were ordered from Sigma Genosys (Oakville, ON).
- 1 ml tubes were stored in CryoBoxes which were then stored in CryoBox vertical racks from Nalgene (Rochester, NY).
- Phenol:Chloroform:Isoamyl Alcohol (25:24:1) was purchased from Invitrogen Life Technologies (Burlington, ON).
- P2, P10, P20, P200, P1000, P5000 Pipetmen from Gilson were supplied by Mandel Scientific Company Inc. (Villiers-le-Bel, France).
- Plasmid Midi Kit, QIAquick PCR Purification Kit and QIAquick Gel Extraction Kit were purchased from Qiagen (Mississauga, ON).
- Yeast extract and granulated agar were purchased from Becton Dickinson and Company (MD).
- Ammonium chloride, disodium hydrogen orthophosphate heptahydrate, glycerol, magnesium sulphate, potassium chloride, sodium dihydrogen orthophosphate, sucrose, sodium hydroxide and D-glucose were purchased from BDH Inc.
- Amicon Ultrafiltration devices, 10K MWCO (15 ml) were purchased from Millipore (Bedford, MA).
- FuGene 6 transfection reagent was purchased from Roche Diagnostics (Laval, QB).
- Hoechst Dye 33342, Mitotracker Red 580, Annexin V 594 (Molecular Probes, USA), and Brain Derived Neurotropic Factor (Alomone Labs, Israel) were kindly obtained from Dr. S. Pandey.
- Geneticin G418 was purchased from Gibco (Burlington, ON).
- Polyclonal rabbit anti-PDI antibody was purchased from Abcam (Cambridge, MA).

Reproduced with permission of the copyright owner. Further reproduction prohibited without permission.

- Anti-goat horseradish peroxidase antibody was kindly obtained from Dr. B. Mutus.

2.2.2 Bacterial Strains and Plasmids

- pET 28b (Novagen).
- pET 11a (Novagen) containing PDI cDNA was kindly obtained from Dr. B. Mutus. It was a gift from X. Jiang.
- pEGFP-N1 (Clontech).
- BL21(DE3) *E.coli* cells (Invitrogen Life Technologies).

2.2.3 Apparatus and Instrumentation

- Acrylamide gels were cast on a Hoefer Mighty Small SE 245 Dual Gel Caster, and acrylamide gel electrophoresis was conducted using a Hoefer Mighty Small II SE 250 Mini-Vertical Gel Electrophoresis Unit, both from Amersham Pharmacia Biotech (Laval, QB).
- Agarose was melted in a 0.6 cubic foot microwave oven from Magnasonic (ON, Canada).
- Gel casting and agarose gel electrophoresis were conducted in a Horizon 58 Horizontal Gel Electrophoresis Apparatus from Gibco BRL Life Technologies (Burlington, ON).
- Samples were weighed on a Mettler AE50 scale from Cambridge Scientific (MA, USA).
- Larger samples were weighed on a Ohaus Compact scale from Ohaus Corporation (NJ, USA).

Reproduced with permission of the copyright owner. Further reproduction prohibited without permission.

- Agarose gels stained with ethidium bromide were viewed and photographed on the AlphaImager 2200 Light Imaging System with AlphaEase software from Alpha Innotech Corporation (San Leadro, CA).
- Agarose gels stained with ethidium bromide were viewed using the Benchtop Ultraviolet Transilluminator from VWR Scientific (ON, Canada).
- The Agilent 8453 UV-visible spectrophotometer from Agilent Technologies (ON, Canada) was used to measure protein concentration, enzyme activity, and cell culture growth and density.
- Polymerase Chain Reactions (PCR) were carried out in a 48-well Perkin Elmer Cetus DNA thermal cycler from Perkin Elmer, (CT, USA).
- Centrifugations were performed using an Fisher Model 59A microcentrifuge from Fisher Scientific (ON, Canada).
- pH measurement of buffers and solutions were done using pH Meter Model 420A by ORION (ON, Canada).
- Insulin turbidity assay was measured on the Ultra Microplate EL_x808_{IU} from BIO-TEK Instruments, Inc. (VT, USA).
- Incubations at 37°C with agitation were done in the C25 Incubator Shaker Classic Series by New Brunswick Scientific Co., Inc.
- Cell lysis was performed using the Sonic Dismembrator Model 100 from Fisher Scientific (ON, Canada).
- Bacteria grown on agar plates were incubated in the Model 1510E Incubator by VWR Scientific (ON, Canada).
- Heating and boiling of protein samples were in the Canlab block heater by American Hospital Supply Canada Inc.
- All microscopy was performed on the Leica DM IRB Microscope from Leica Microsystems (Germany).

Reproduced with permission of the copyright owner. Further reproduction prohibited without permission.

- All pictures were taken using a QImaging camera.
- DCFDA fluorescence was measured with the Spectra Max Gemini XS multi-well plate fluorescence reader (CA, USA).
- Centrifugation was performed on a J2-HS Beckman centrifuge with JA-10, JA-14, and JA-20 rotors.
- Ischemic conditions were simulated with the Gas Pack System from Becton Dickenson (Cockeysville, MD).
- Dessication of protein was done in the Labconco Model 4451F Lyophilizer, Labquip Limited (Markham, ON).
- DNA sequencing was performed at Wayne State University DNA Sequencing facility.

2.2.4 Cell Lines and Media

Human umbilical vein endothelial cells (HUVEC) were purchased from the American Type Culture Collection (ATCC), and were maintained in Kaighn's F12K medium (Gibco, Canada) containing 1.5 g/L sodium bicarbonate, 2 mM L-glutamine, and supplemented with 0.1 mg/ml heparin (Sigma, Canada), 10% fetal bovine serum (Gibco, Canada), and 0.03-0.05 mg/ml endothelial cell growth supplement (BD Biosciences, USA). Human Neuroblastoma (SH-SY5Y) cells were also purchased from ATCC, and maintained in Dulbecco's Modified Eagle Medium Ham's F12 media (Sigma, Canada) containing 1.5 g/L sodium bicarbonate, and supplemented with 10% fetal bovine serum (Gibco, Canada), and 2 mM L-glutamine (Gibco, Canada).

2.2.5 General Decontamination and Sterilization Procedures

All glassware, pipette tips, centrifuge tubes, and Milli-Q water used for both bacterial and mammalian cell culture were autoclaved to avoid bacterial and fungal contamination. All supplies used in the cell culture laminar flow hood were sprayed

Reproduced with permission of the copyright owner. Further reproduction prohibited without permission.

with 70% ethanol. The laminar flow hood was sterilized each day with an ultraviolet lamp.

2.3 Protein and Bacterial Work

2.3.1 PDI cDNA Expression Cloning in Bacterial Cells

The plasmid vector pET-11a containing PDI cDNA, was verified by sequencing prior to use for cloning. An expression construct was derived using *Taq* polymerase and primers (forward 5-AAAGAATTCAGACGCCCCCGAGGAGGAGGAC-3; reverse 5-CCCAGGCTTCAGTTCATCTTTCACAGCTTTCTGATC-3) which bracketed the open reading frame of PDI cDNA and possessed restriction sites for *Eco RI* and *Hind III*, respectively, to facilitate insertion into pET-28b. Primers were generated by Sigma Genosys and designed by the custom created computer program written by R. Nistor and D. Seslija found in Appendix C. Polymerase chain reaction was carried out in a total volume of 100 μl, containing 20 mM ammonium sulfate, 75 mM Tris-HCl (pH 8.8), 5 mM $MgCl_2$, 20 μM of each dNTP, 50 pmol of each primer, 500 ng of pET-11a template, and 2 units of *Taq* DNA polymerase. PCR was run for 30 cycles (95°C for 60 seconds, 55°C for 30 seconds, 72°C for 80 seconds. Samples were stored at 4°C until further use (Gibbs, 1990). The insert and vector were ligated together using T4 DNA ligase, according to directions by Promega. The construct was transformed into *E. coli* strain BL21(DE3) using the calcium chloride protocol (Sambrook *et al.*, 1989) and grown on agar plates containing 10 mg/L of kanamycin. The presence of PDI cDNA insert in bacterial cells was then verified by screening colonies from the plates, followed by plasmid extraction (Novagen pET manual protocol) and digestion with the restriction enzymes *EcoRI* and *HindIII*. The restriction digest was analyzed on a 1.5% agarose gel (Sambrook *et al.*, 1989). Wayne State University DNA Sequencing facility verified the presence of the fusion product.

Reproduced with permission of the copyright owner. Further reproduction prohibited without permission.

2.3.2 PDIa cDNA Expression Cloning in Bacterial Cells

An expression construct was derived using *Taq* polymerase and primers (forward 5-AAAGAATTCAGACGCCCCCGAGGAGGAGGACCACGTCCTG-3; reverse 5-TT TAAGCTTGGCAGCCGGGCCCGTGCGCTTCTTCAGCCA-3) which bracketed the open reading frame of the active site a domain (PDI-a), and possessed restriction sites for *EcoRI* and *HindIII*, respectively, to facilitate insertion into pET-28b (refer to Appendix B). Primer construct and PCR were done as described in section 2.3.1. The insert and vector were ligated and transformed into *E. coli* BL21(DE3). Cells were maintained on agar plates containing 10 mg/l kanamycin plates. The presence of the a-domain was verified by sequencing at the Wayne State University DNA sequencing facility.

2.3.3 Purification of the Recombinant Proteins

Bacterial cultures containing the recombinant plasmid were induced with 1 mM IPTG overnight at room temperature. Cultures were centrifuged at 6 000 rpm in a JA-10 rotor for 20 minutes at 4°C and the supernatant was discarded. The pellet was resuspended in cell lysis buffer (3 ml/g of pellet). Lysozyme was added to the suspension to a final concentration of 0.3 mg/ml and shaken at 4°C for 30 min. Sodium deoxycholate (1 mg/ml), DNase I (6.7 mg/L), and RNase (6.7 mg/L) were added to the lysate and shaken at 37°C for 20 minutes, until the mixture was no longer viscous. The cell suspension was sonicated 3 times for 30 seconds at level 7.5 on the Sonic Dismembrator, and the mixture was then centrifuged at 15 000 rpm on a JA-20 rotor for 20 min at 4°C. The pellet was kept on ice, while the supernatant was added to the nickel column. The recombinant fusion protein was isolated using nickel affinity chromatography. All steps were performed at 4°C unless otherwise stated. Prior to loading the crude extract, 1.5 ml of nickel resin suspension was prepared according to the Sigma product manual protocol. The crude extract was then shaken gently at 4°C for 30 minutes. The crude extract-resin mixture was then packed into a 20 ml polypropylene column and loaded at a flow rate of 1 ml/min. The flow through

Reproduced with permission of the copyright owner. Further reproduction prohibited without permission.

was collected and reserved for SDS-PAGE. The resin was then washed with 30 ml of 10 mM imidazole wash buffer or until the optical density (OD) measured at 595 nm was comparable to the blank. The resin was then washed with 30 ml of 30 mM imidazole, or until the OD_{595} was similar to the blank. Further non-specifically bound proteins were washed with 10 ml of 100 mM imidazole, and finally, the target protein was eluted within the first 4 ml of 250 mM imidazole elution. The eluted protein was collected in 1 ml fractions, and its concentration was determined using the Bradford reagent. To confirm the presence of the isolated his-tagged protein, PDI, and PDI-a were analysed together on a 13.5% SDS-PAGE and then stained with Coomassie blue.

2.3.4 Immunoblot Analysis

Purified recombinant protein was run on a 13.5% SDS-PAGE gel, and electrophoretically transferred to nitrocellulose membrane using transfer buffer (20% methanol, 24 mM tris base, 0.2 M glycine)(Sambrook *et al*, 1989). After transfer, the blot was temporarily stained with a 1:9 dilution of Ponceau S for 10 minutes, and washed with water. The blot was placed in Tris Buffered Saline (TBS - 0.02 M Tris HCL, 0.2 M NaCl, pH 8.2) solution with 5% skim milk for 2 hours at room temperature, to block non-specific binding sites on the membrane. Incubation with primary polyclonal rabbit anti-PDI antibodies at a 1:1000 dilution in TBS with 2% skim milk was done overnight at 4°C. The membrane was then washed with TBS twice for 10 minutes. For detection of polyclonal anti-PDI antibody, the membrane was incubated with the secondary antibody horseradish peroxidase anti-goat IgG at a 1:2000 dilution in TBS with 2% skim milk at 4°C for 2 hours. The membrane was then washed for 30 minutes with TBS. Visualization was performed by adding 5 ml of 3',3',5',5'-Tetramethylbenzidine producing a permanent blue reaction product.

2.3.5 Insulin Turbidity Assay

To test the activity of both recombinant proteins, the experiment described by Holmgren (1979) was modified for a 96-well plate. 4 mM DTT, 2 μM enzyme sample,

Reproduced with permission of the copyright owner. Further reproduction prohibited without permission.

and 1 mM insulin were added to the assay buffer (0.1 M K_2HPO_4, 2 mM EDTA, pH 7.0) to a volume of 200 μl. Absorbance was monitered using the kinetics mode at 650 nm at 0.5 minute intervals for 30-45 minutes.

2.3.6 PDI cDNA Expression Cloning in Bacterial Cells for Mammalian Expression

An expression vector for protein localization was derived using *Taq* polymerase and forward primers 5-AAAAGAATTCTTATGGACGCCCCCGAGGAGGACGAC-3; reverse primer 5-AAATGGTACCTGCAGTTCATCTTTCACAGCTTTCTGATC-3) which bracketed the open reading frame of the PDI cDNA, and possessed restriction sites for *Eco RI* and *Kpn I*, respectively, to facilitate insertion into pEGFP-N1 (refer to Appendix B). The insert and vector were ligated and transformed into *E. coli* BL21(DE3) as described previously in section 2.3.1. Cells were maintained on agar plates containing 10 mg/L kanamycin. The construct was also verified through sequencing by Wayne State University DNA Sequencing facility.

2.3.7 HUVEC Transient Transfection

A standard protocol for calcium phosphate-mediated transfection (Sambrook *et al.*, 1989) was performed on the HUVECs. Plasmids pEGFP-N1 and PDI:pEGFP-N1 were prepared using the Qiagen midiprep kit, and DNA concentration and purity were measured at an absorbance of 260 nm and 280 nm (Glasel, 1995). Visualization of the plasmid DNA was executed on a 1.5% agarose gel. HUVEC transfection was also attempted using FuGENE 6 transfection reagent, according to the manufacturer's protocol (Roche Diagnostics).

Reproduced with permission of the copyright owner. Further reproduction prohibited without permission.

2.3.8 *In Vitro* Transfection by a Liposomal reagent in SH-SY5Y Cells

FuGENE 6 transfection reagent was used to transfect SH-SY5Y cells, according to the manufacturer's protocol (Roche Diagnostics). pEGFP-N1 and PDI:pEGFP-N1 plasmids were prepared using the Qiagen midiprep kit, and DNA concentration and purity was measured as described in section 2.3.7. Success of transfection was verified by observation of the green fluorescence of cells under a UV lamp with a GFP filter.

2.3.9 Determination of G418 Sensitivity on SH-SY5Y Cells

A set of eight (35 mm^2 x $10mm^2$) plates were prepared by splitting a confluent 25 mm^2 flask so the cells were 25% confluent in 24 hours. The next day the culture medium was replaced with medium containing varying concentrations of G418 (0, 50, 150, 200, 300, 400, 500, 800 μg/ml G418). G418 was used to select against cells that did not contain the pEGFP-N1 plasmid. The selective media was changed every 48 hours, and the percentage of surviving cells was observed. The concentration of antibiotic G418 that prevented cell growth within two weeks was chosen (Tzen *et al*, 1990).

2.3.10 Generation of a Stable Cell Line in SH-SY5Y Cells

Two sets of SH-SY5Y cells were transfected with either pEGFP-N1 plasmid, or PDI:pEGFP-N1 plasmid. Forty-eight hours post transfection, the cells were split into a 1:3 ratio, with medium containing the 200 μg/ml of G418. The cells were fed with selective medium every 48 hours for one week, until colonies of stable cells were identified with fluorescent microscopy. Cells were then transferred into 24-well plates for growth and expansion.

Reproduced with permission of the copyright owner. Further reproduction prohibited without permission.

2.3.11 Effect of Coenzyme Q_{10} (CoQ_{10}) on Improving the Lifetime of Stable Cells

Following the generation of stable cell lines, cells were lifted from the 24-well plate, and transferred to 35 mm^2 x $10mm^2$ plates. 1 μl of CoQ_{10} (50 mg/ml) was added for each millilitre of media, for half of the plates. Cells were examined for vitality and the absence of senescent cells, in comparison to those plates without CoQ_{10}.

2.3.12 Preparation of the Total Cell Lysate

Following experimental assays, the cells were washed twice with 1 X PBS, pH 7.4, and then incubated at 4°C with TNTE buffer (0.5% Triton X, 150 mM NaCl, 50 mM Tris, pH 7.5, 1 mM EDTA) for 15 minutes. Cells were harvested by mechanical dislodging with a rubber policeman, and the lysate was spun at 5 000 rpm in a JA-20 rotor for 5 minutes. The supernatant was removed, and the pellet was resuspended in 200 μl of TNTE buffer containing 10 μl of protease inhibitor cocktail (prepared as described in the Sigma product information). The concentration of the total cell lysate was estimated using the Bradford reagent at an absorbance of 595 nm.

2.3.13 Immunoprecipitation

Cells were lysed as described previously (section 2.3.12), and the concentration of protein used was 1 mg/ml. Polyclonal rabbit anti-PDI antibodies were added to the total cell lysate to a dilution of 1:100. The mixture was incubated on ice for two hours. Approximately 50 μl of Protein A agarose beads were added for every 200 μl of cell lysate, and the solutions were rocked at 4°C for two hours. The beads were collected by microcentrifugation at maximum speed and washed three times with 1 ml of TNT buffer (same as TNTE minus the EDTA). The supernantant was removed, and the beads were resuspended in 50 μl of 2X loading buffer, and boiled for 5 minutes at 100°C. Products were loaded onto a 10% SDS-PAGE gel, and subjected to a Western blot.

Reproduced with permission of the copyright owner. Further reproduction prohibited without permission.

2.3.14 SH-SY5Y Differentiation

Differentiation of SH-SY5Y cells were carried out using a previously described method (Encinas *et al.*, 2000). Cells were plated in 35 mm^2 petri plates, pre-coated with 0.05% collagen. Twenty-four hours later, *all-trans* retinoic acid was added to a final concentration of 10 μM, in F12 medium containing 15% Fetal Bovine Serum for 5 days. Following, the cells were washed twice with F12 medium and incubated with 50 ng/ml Brain Derived Neurotropic Factor (BDNF) in serum free media for seven days.

Reproduced with permission of the copyright owner. Further reproduction prohibited without permission.

2.4 Results

2.4.1 Development and Expression of PDI in Bacteria

To clone the sequence of full length PDI (approximately 1490 nucleotides) into pET-28b, amplification of the human PDI cDNA sequence was performed from the pET-11a vector containing PDI cDNA, using PCR with primers flanking the cDNA sequence of PDI (figure 2.1). Bands of approximately 1.5 Kilobases (Kb) were identified to be amplified PDI cDNA. Two bands of 0.38 Kb and 0.05 Kb were found and indicate non-specific primer binding, due to the identical sequences of the a and a' domain. Annealing temperatures of 55°C (lane 2) and 60°C (lane 3) were used in the PCR reactions. There was no major difference in PCR product with the five degree temperature differential. PCR cDNA from lane 3, at a molecular weight of 1.5 Kb, was used for ligation to the pET-28b vector.

Following ligation of the insert to the vector, colony screening and restriction enzyme digestion was done with *EcoRI* and *HindIII*. The band observed at 1.5 Kb indicated the presence of PDI cDNA in the pET-28b vector (lane 4 - figure 2.2). The 5.4 Kb band in lane 4 of figure 2.2 was the pET-28b plasmid. Lane 2 indicates the molecular weight of pET-28b plasmid, which is 5.4 Kb. Bands located higher than the molecular weight ladder indicate a linear conformation of the plasmid, as opposed to its coiled or supercoiled forms which migrate more easily through the gel. Lane 3 indicates the the observed molecular weight of the ligated pET-28b:PDI plasmid which is 6.9 Kb. The digested pET-28b:PDI plasmid in lane 4 clearly indicates the molecular weight of the cDNA as 1.5 Kb.

The sequence of the reading frame from the 1.5 Kb piece of DNA of the recombinant plasmid was aligned with the cDNA sequence originally obtained from the pET-11a:PDI plasmid,and GenBank accession number E03087 (human PDI) giving 99.8% sequence identity. Base pair differences were due to the lack of identification of some base pairs, due to signal weakness, and lack of base pair identification in the chromatograph obtained from the Wayne State sequencing facility. The DNA sequence was consistent with the correct protein sequence.

Reproduced with permission of the copyright owner. Further reproduction prohibited without permission.

Similarily, cDNA amplification specific to the a domain (approximately 380 nucleotides) of PDI yielded bands of 0.38 Kb (figure 2.3). Again, non-specific primer binding was present in both lanes, as indicated by the additional bands found at 0.05 Kb. Colony screening and restriction enzyme digestion showed the presence of the 0.38 Kb insert in the pET-28b vector (lane 2 - figure 2.4). Sequence identity between the a domain and full length PDI yielded 99.3% identity. Base pair differences were due to the lack of identification of some base pairs, due to signal weakness in the chromatograph obtained from the Wayne State sequencing facility.

Expression of each recombinant protein yielded approximately 18 - 25 mg of protein per 1 litre of bacterial culture. The presence of full-length PDI and PDIa protein were visualized by bands of approximately 66 KDa, and 19 KDa respectively (lane 7 - figure 2.5, lane 6 - figure 2.6). The increase in molecular weight by approximately 9.5 KDa of both recombinant proteins was due to the presence of both an N-terminal and C-terminal His_6 tags. Removal of the N-terminal His-tag would theoretically result in molecular weights of 61 KDa for full length PDI, and 14 KDa for the active site domain.

A Western blot further confirmed the presence of PDI and PDIa (lanes 1 and 2 - figures 2.7 and 2.8). Repeated detection of a weak band at twice the molecular weight (132 KDa) of full-length PDI agrees with the assumption of native PDI existing as a homodimer (Noiva, 1999). The insulin turbidity assay (figure 2.9) indicates that the activity of the full-length recombinant PDI is comparable to that of Sigma bovine PDI; the activity of the a domain showed comparable results, based on its capacity as a single domain. Removal of the N-terminal His_6 tag through cleavage with thrombin, but its removal was found to have no effect on the activity of the protein (data not shown).

Reproduced with permission of the copyright owner. Further reproduction prohibited without permission.

2.4.2 Development, Expression, and Localization of PDI in SH-SY5Y Cells

To develop a live cell reporter protein system constitutively expressing PDI, N-terminal fusion of full-length human PDI to GFP was done using vector pEGFP-N1 (Clontech). Using primers flanking full-length PDI, PCR was used to amplify its sequence from the pET-11a vector (lane 2 - figure 2.10). A band of approximately 1.5 Kb was identified to be PDI cDNA. Bands found at 0.38 Kb and 0.05 Kb were again considered to result from non-specific primer binding. Following ligation of the 1.5 Kb insert to the pEGFP-N1 vector, colony screening followed by restriction enzyme digest with enzymes *EcoR1* and *KpnI*, indicated the presence of the 1.5 Kb full length PDI cDNA within the vector (lane 4 - figure 2.11). Sequence alignment of the experimentally determined reading frame from this recombinant plasmid was compared with the cDNA sequence obtained from the pET-11a:PDI plasmid, giving a 97.6% sequence identity. Base pair differences were due to the lack of identification of some base pairs, due to signal weakness in the chromatograph obtained from the Wayne State sequencing facility. There was no noticeable effect on the protein sequence.

HUVEC cells were chosen initially chosen as the target of mammalian cell transfection, based on their role in nitric oxide transport. However, attempts using both calcium phosphate, and liposomal (FuGene) mediated transfection were unsuccessful, based on the transfection efficiency of this particular cell type. Instead, transient and stable cell lines of SH-SY5Y neuroblastoma cells were generated using FuGene 6 transfection reagent. Cells were maintained at a concentration of 200 μg/ml of G418, and it was found that the addition of 0.05 mg/ml of CoQ_{10} had no noticeable effects on reducing the number of senescent cells after 10 population doublings. Presence of the reporter protein in SH-SY5Y cells was verified by immunoprecipitation (figure 2.12). The molecular weight of GFP alone is approximately 27 KDa, and the molecular weight of PDI alone is approximately 57 KDa, together, with the presence of a small linker region between the two proteins, yields a molecular weight of approximately 87 KDa. The 87 KDa band visible in lane one of figure 2.12 shows the presence of

Reproduced with permission of the copyright owner. Further reproduction prohibited without permission.

the PDI:GFP reporter protein in the transfected cells. The band at approximately 57 kDa identifies the endogenous level of PDI found in the cells. Protein localization of PDI was examined in a stable cell line of differentiated SH-SY5Y cells. Cells were observed for areas of green fluorescence, which was found throughout the cell, including the cytoplasm and dendrites (figure 2.13). Green fluorescence was also observed within the nucleus, and arrows indicate the absence of PDI:GFP in the nucleoli of the cells.

Reproduced with permission of the copyright owner. Further reproduction prohibited without permission.

2.5 Discussion

The study of protein structure and function has been greatly aided by the development of systems that are able to regulate protein expression. More specifically, recombinant protein systems allow for the controlled expression of copious amounts of proteins, otherwise too difficult to obtain from their natural *in vivo* conditions. Full-length PDI and its active site domain were produced in *E. coli* as soluble proteins, with the addition of 2 His_6 tags located at the N and C-termini of each protein, to aid in purification. The isolated recombinant full-length PDI exhibited enzymatic activity similar to commercially available bovine PDI, as verified with the insulin turbidity assay. Enzymatic activity of the active site domain a showed a functional protein, but only at a 61% level of the full length protein. Kinetic parameters cannot be deduced from the insulin assay under these conditions, as it was just used to test the relative activity of the protein for functionality purposes. The characterization of the functional properties of both a and a' domains in work by Darby and Creighton in 1995, compared the activity in the reactivation of disulfide-scrambled ribonuclease A, disulfide folding of BPTI, and disulfide formation in model peptides. In these instances, the two active site domains were shown to be efficient in their ability to introduce disulfide bonds in unfolded proteins, but were less efficient than full length PDI in disulfide bond isomerization. The engineering of a recombinant full-length PDI was created to assist the study and characterization of the S-nitrosation activity of PDI. It was shown that PDI denitrosates S-nitrosoglutathione (GSNO), and that by auto-S-nitrosation of the active site through N_2O_3, PDI can act as a NO carrier (Sliskovic *et al.*, 2005).

In studying PDI kinetics, it has been difficult to estimate initial rates of enzyme turnover. It has also been difficult to determine Michaelis-Menten parameters of PDI; enzyme rates increase as enzyme concentration is increased, and there are long lag phases before reactions are detectable. Many models of its mechanism have been proposed, but all lack experimental evidence to support them. In a study by Raturi and coworkers (2005), a more sensitive assay for PDI was developed, based on the

Reproduced with permission of the copyright owner. Further reproduction prohibited without permission.

PDI-dependent reduction of a synthetic fluorescent self-quenching probe di (*o*-amino benzoyl) glutathione disulfide (*diabz*-GSSG). The reduction of *diabz*-GSSG to (*O*-amino benzoyl)-glutathione (*abz*-GSH) by PDI results in an increase in fluorescence; it utilizes low concentrations of PDI, in an immediate reaction that can easily be monitered spectroscopically.

Coenzyme Q10 is the electron transporter in the mitochondrial respiratory chain, and has been shown to reduce apoptosis (Moon *et al.*, 2005). Addition of coenzyme Q10 to the cell media was done as an attempt to preserve transfected cells, and delay senesence of the stably transfected cells. Unfortunately, no noticeable differences were seen in generating and maintaining stable cell lines between those cells receiving 0.05 mg/ml of coenzyme Q10, and the cells receiving no extra treatment in its place. Although traditionally thought of as an enzyme localized specifically to the ER, more recent studies have shown that PDI is found throughout the cell. Cell surface PDI was identified on the surface of human blood platelets (Chen *et al.*, 1995), mitochondrial PDI was found in rat liver cells (Rigobello *et al.*, 2000), and PDI has been located throughout the cytosol in astrocytes of glial cells (Safran *et al.*, 1991). In this study, the localization of PDI in differentiated human neuroblastoma cells shows the dispersal of PDI throughout the cell, and into the dendridic arms, indicating that it is not only localized to the ER in SH-SY5Y cells. Implications for the potential purpose of this protein throughout the cytosol of these cells is discussed in section 3.4.

Reproduced with permission of the copyright owner. Further reproduction prohibited without permission.

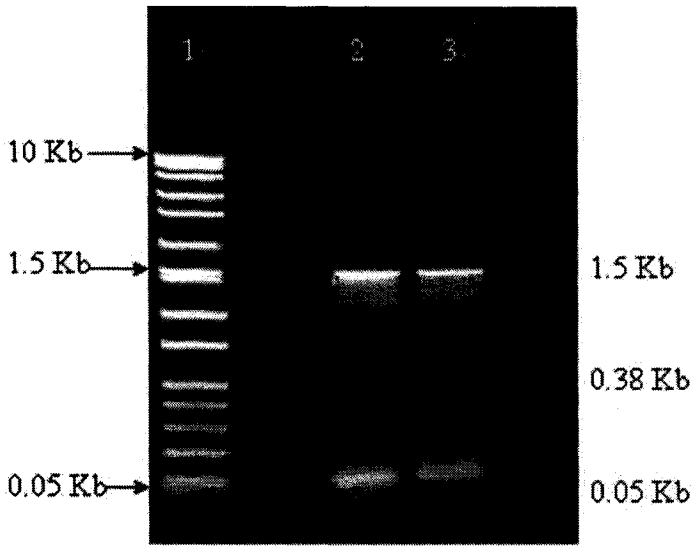

Figure 2.1: cDNA amplification of full-length PDI. An image of the 1.5% agarose gel resolution of the PCR products. Lane 1 contains a DNA marker ranging from 10 Kb to 0.05 Kb. Lane 2 contains amplified PDI cDNA under an annealing temperature of 55°C, and lane 3 contains amplified PDI cDNA under an annealing temperature of 60°C.

Reproduced with permission of the copyright owner. Further reproduction prohibited without permission.

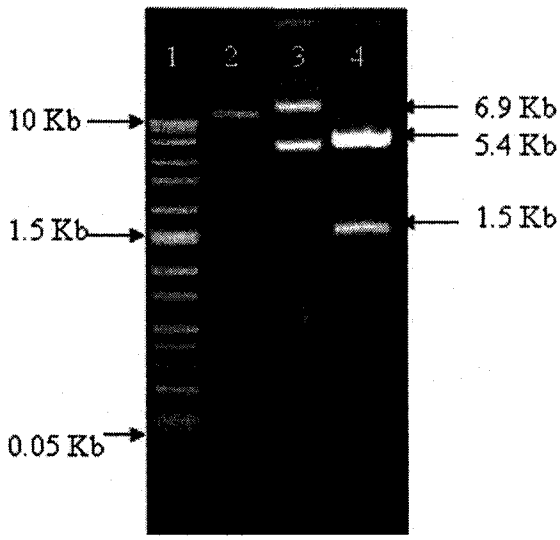

Figure 2.2: pET-28b:PDI fusion and restriction enzyme digest. An image of the 1.5% agarose gel resolution of the plasmid extraction and restriction enzyme digest products. Lane 1 contains the DNA marker, lane 2 contains pET-28b plasmid, lane 3 contains recombinant pET-28b:PDI, and lane 4 contains the restriction enzyme digest of pET-28b:PDI by restriction enzymes *EcoR1* and *HindIII*.

Reproduced with permission of the copyright owner. Further reproduction prohibited without permission.

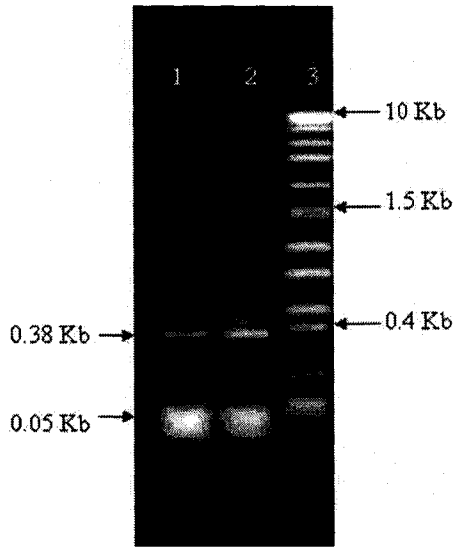

Figure 2.3: cDNA amplification of the active site domain of PDI. An image of the 1.5% agarose gel resolution of the PCR products. Lane 1 contains amplified PDI cDNA under an annealing temperature of 55°C, lane 2 contains amplified PDI cDNA under an annealing temperature of 60°C, and lane 3 contains the DNA marker.

Reproduced with permission of the copyright owner. Further reproduction prohibited without permission.

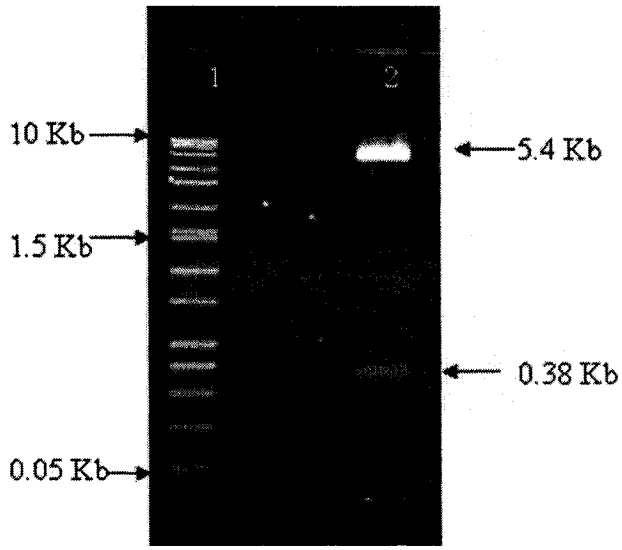

Figure 2.4: pET-28b:PDIa fusion and restriction enzyme digest. An image of the 1.5% agarose gel resolution of the restriction enzyme digest products. Lane 1 contains the DNA marker, lane two contains the restriction enzyme digest of pET-28b:PDIa by restriction enzymes *EcoR1* and *HindIII*.

Reproduced with permission of the copyright owner. Further reproduction prohibited without permission.

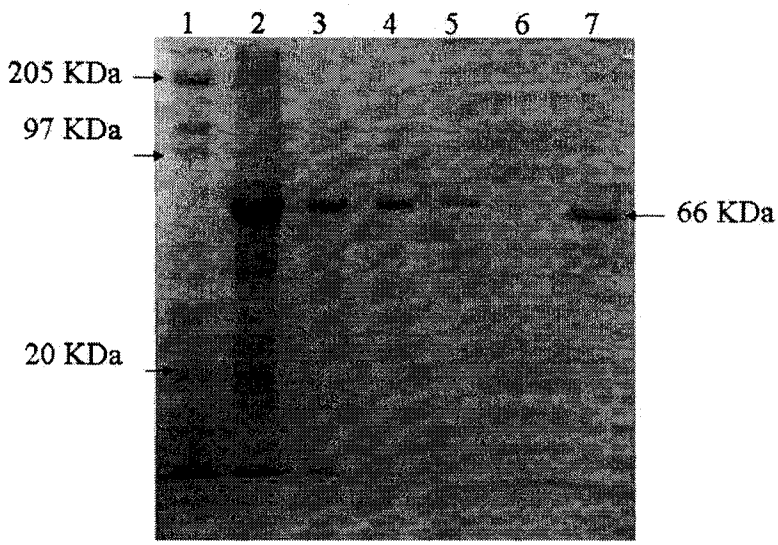

Figure 2.5: Protein purification of recombinant PDI. An image of a 12% acrylamide gel containing recombinant PDI. Lane 1 contains the molecular weight (MW) markers ranging from 205 KDa to 6.5 KDa. Lane 2 contains protein eluted with 10 mM imidazole; lane 3 contains a second elution with 10 mM imidazole; lane 3 contains a third 10 mM imidazole wash; lane 4 contains protein eluted with 30 mM imidazole; lane 5 contains a second 30 mM wash, and lane 6 contains recombinant protein eluted with 250 mM imidazole.

Reproduced with permission of the copyright owner. Further reproduction prohibited without permission.

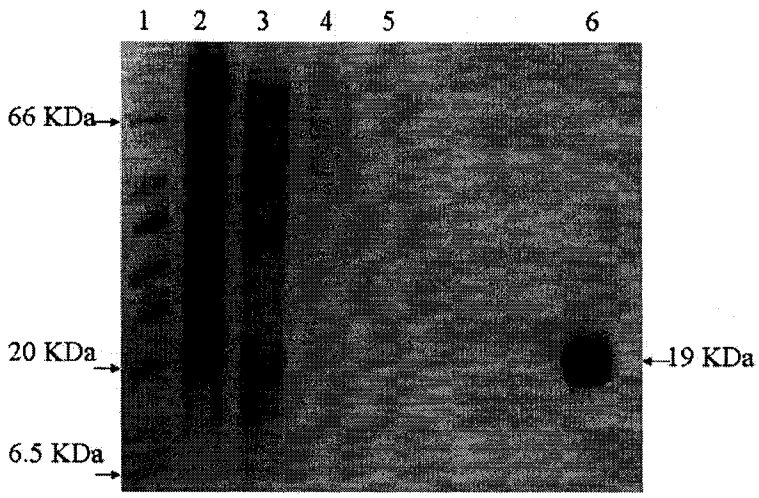

Figure 2.6: Protein purification of recombinant PDIa. An image of a 17% acrylamide gel containing recombinant PDIa. Lane 1 contains a MW marker ranging from 66 KDa to 6.5 KDa. Lane 2 contains insoluble proteins in the pellet; lane 3 contains proteins eluted with a 10 mM imidazole wash; lane 4 contains a second 10 mM imidazole wash; lane 5 contains proteins eluted with a 30 mM imidazole wash, and lane 6 contains recombinant protein eluted with 250 mM imidazole.

Reproduced with permission of the copyright owner. Further reproduction prohibited without permission.

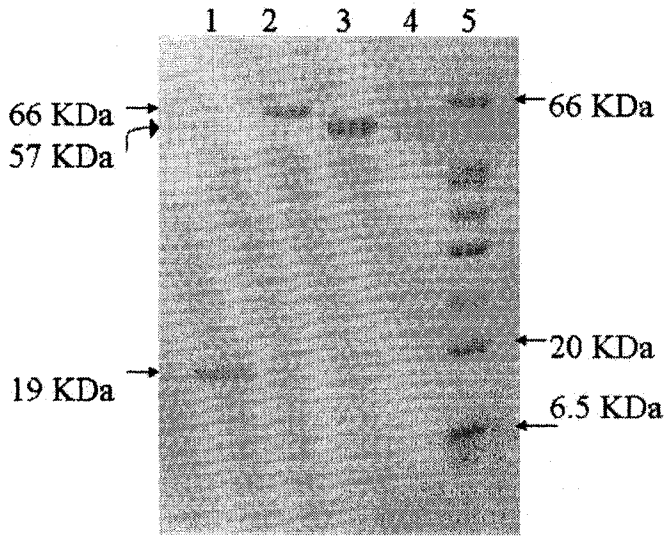

Figure 2.7: Ponceau-S stain of nitrocellulose prior to immunoblotting. Lane 1 contains recombinant PDIa protein; lane 2 contains recombinant PDI protein; lane 3 contains Sigma bovine PDI; lane 4 contains Bovine Serum Albumin (BSA), and lane 5 contains a MW marker ranging from 66 KDa to 6.5 KDa.

Reproduced with permission of the copyright owner. Further reproduction prohibited without permission.

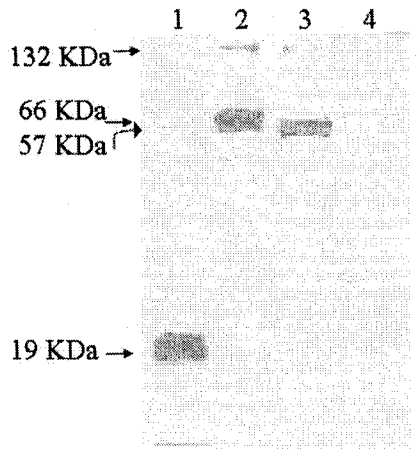

Figure 2.8: Western blot of PDI and PDIa. An image of the colorimetric development by 3',3',5',5'-Tetramethylbenzidine after immunoblotting. Lane 1 contains recombinant PDIa protein; lane 2 contains recombinant full length PDI with 2 His_6 tags; lane 3 contains Sigma bovine PDI (positive control), and lane 4 contains BSA (negative control).

Reproduced with permission of the copyright owner. Further reproduction prohibited without permission.

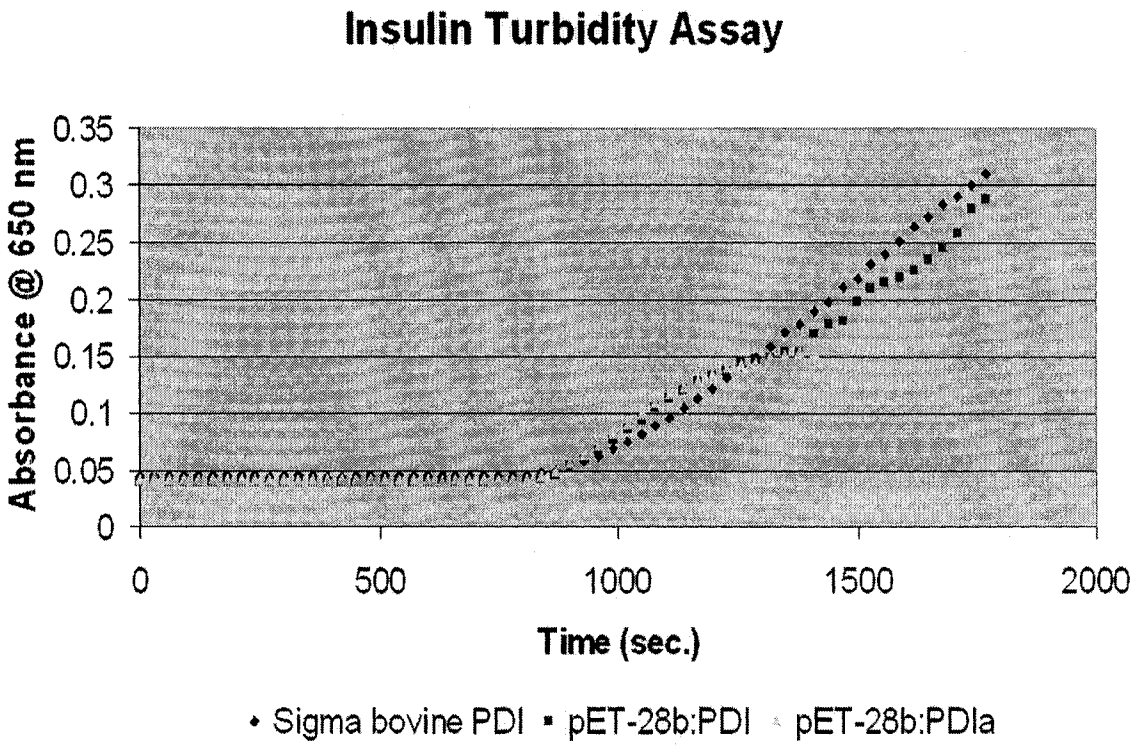

Figure 2.9: Insulin turbidity assay of the recombinant proteins. Sigma bovine PDI and recombinant human PDI show similar enzymatic activity. Recombinant PDIa is active, but its activity is decreased in comparison to full-length PDI.

Reproduced with permission of the copyright owner. Further reproduction prohibited without permission.

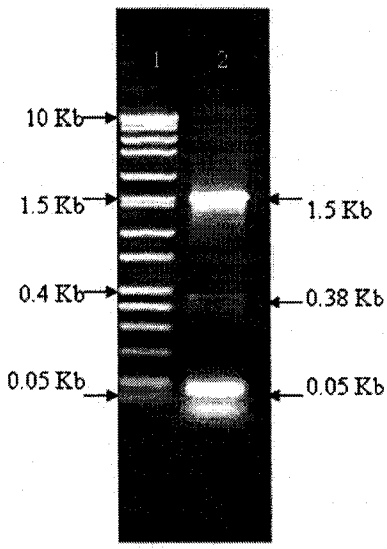

Figure 2.10: cDNA amplification of full-length PDI. An image of the 1.5% agarose gel resolution of the PCR products. Lane 2 contains amplified PDI cDNA under an annealing temperature of 55°C, and lane 1 contains the DNA marker.

Reproduced with permission of the copyright owner. Further reproduction prohibited without permission.

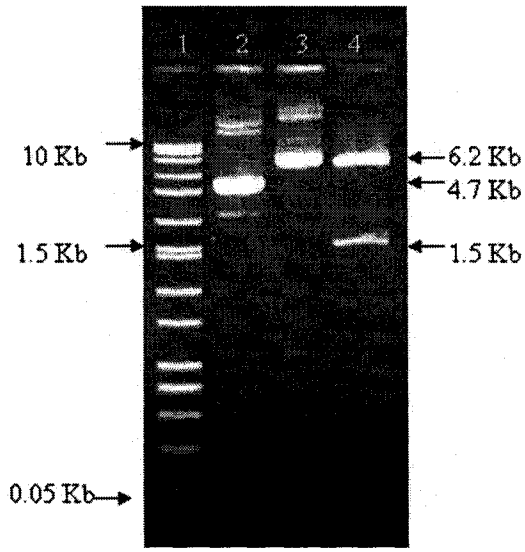

Figure 2.11: pEGFP-N1:PDI fusion and restriction enzyme digest. An image of the 1.5% agarose gel resolution of the plasmid extraction and restriction enzyme digest products. Lane 1 contains the DNA marker; lane 2 contains plasmid pEGFP-N1; lane 3 contains recombinant plasmid pEGFP-N1:PDI. In lanes 2 and 3 the linear, coiled, and supercoiled forms of the plasmid are observed. Lane 4 contains the restriction enzyme digest of plasmid pEGFP-N1:PDI by restriction enzymes *EcoR1* and *KpnI*.

Reproduced with permission of the copyright owner. Further reproduction prohibited without permission.

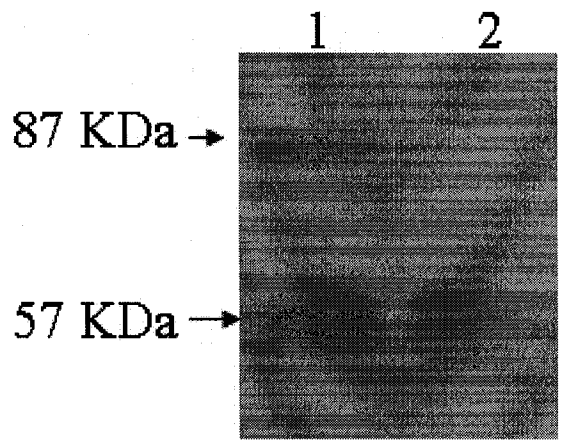

Figure 2.12: Immunoprecipitation of SH-SY5Y cells expressing the reporter protein. Lane 1 contains immunoprecipitation of the total cell lysate from transiently transfected SH-SY5Y cells. Lane 2 contains the control immunoprecipitation of the total cell lysate from untransfected SH-SY5Y cells.

Reproduced with permission of the copyright owner. Further reproduction prohibited without permission.

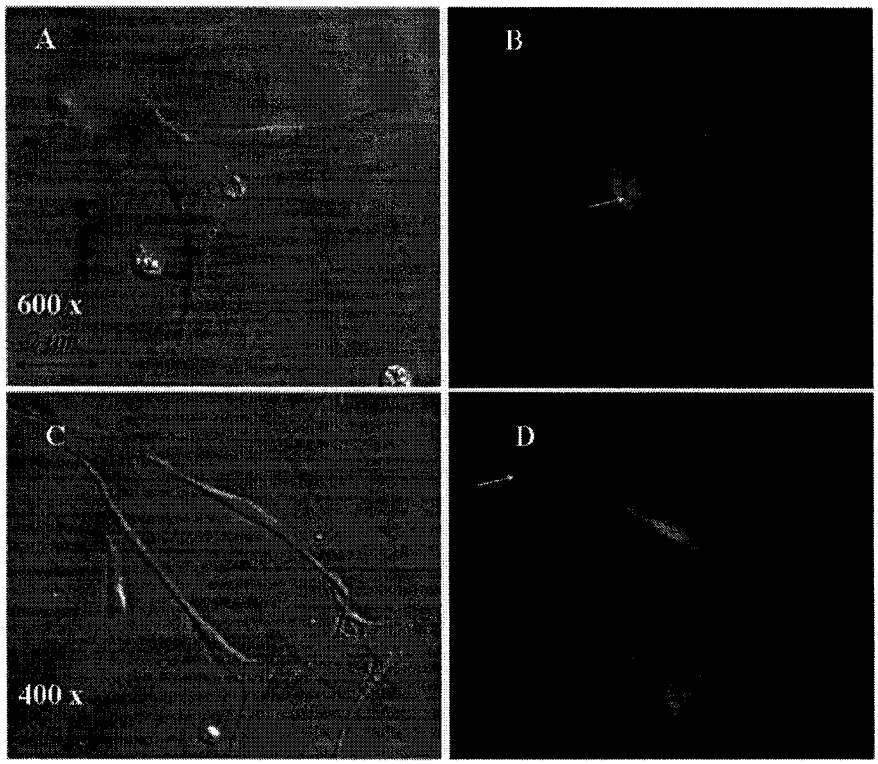

Figure 2.13: Localization of PDI in differentiated SH-SY5Y cells. Photos above (A and B) and below (C and D) compare cell morphology and reporter protein localization of selected cells. Photos A and C were taken under phase contrast microscopy, whereas photos B and D were taken under a fluorescent microscope, containing a blue UV filter. Arrows shown in B and D indicate the absence of PDI:GFP in the nucleoli of the cells.

Reproduced with permission of the copyright owner. Further reproduction prohibited without permission.

Chapter 3

Further Evidence of PDI as a Neuroprotective Protein

3.1 Objectives

In various stressful situations, PDI has been shown to be upregulated. For example, in primary cultured glial cells, the protein was upregulated under hypoxic/ischemic conditions (Tanaka *et al.*, 2000). Overexpression was also demonstrated in the brains of patients with CJD (Yoo *et al.*, 2002). In the previous chapter the localization of the protein in SH-SY5Y cells was probed by creating a PDI:GFP construct. To investigate further the properties of PDI as a neuroprotective protein, stable lines of SH-SY5Y cells were generated containing the PDI:GFP construct. The promoter under which gene expression was controlled was the cytomegalovirus immediate early (CMV IE) promoter, which is constitutively active. In introducing excess PDI to SH-SY5Y cells, it was anticipated that a similar outcome demonstrated by Tanaka, would occur under stressful conditions, and work to protect the cells. Furthermore, Bruening and coworkers (1998) identified that the activation of stress-activated mitogen activated protein kinases (MAPK) upregulated the expression of transgenes under control of the CMV IE promoter, and during ischemic stress members of the MAPK family are activated (Moriya *et al.*, 2000). If the CMV IE promoter is activated through cell stress, then the PDI:GFP construct would be over-

Reproduced with permission of the copyright owner. Further reproduction prohibited without permission.

expressed in the stable cell lines. This chapter sets out to examine further evidence of PDI as a neuroprotective protein under conditions of oxidative and ischemic stress in SH-SY5Y cells.

3.2 Methods

3.2.1 Inducing Oxidative Stress by H_2O_2 Treatment

Oxidative stress was induced by adding H_2O_2 to a final concentration of 100 μM to the untransfected control cells, and to the pEGFP-N1 and PDI:pEGFP-N1 transfected cells. After one hour, the media was changed, and the plates were incubated for three hours at 37°C, 5% CO_2. Apoptotic assays followed three hours after the treatment (Naderi *et al.*, 2003).

3.2.2 Inducing Hypoxia

Cell media was replaced with a controlled salt solution (110 mM NaCl, 5.4 mM KCl, 0.8 mM $MgCl_2$, 1.8 mM $CaCl_2$, 15 mM $NaHCO_3$, 15 mM glucose, 15 mM hepes, and 50 mM glycine, pH 7.4). Cells were put in a Gas Pack (anaerobic vessel) with a catalyst that consumed the remaining oxygen in the tank. An anaerobic indicator was used to moniter the decrease in oxygen. The cells were left in the tank for 6 hours, and media was changed (Munir *et al.*, 1995). The cells were monitered by counting the number of live cells per 100 in three different areas in 35 mm^2 plates over a 48 hour time period. Three trials were done and three sets of measurements were taken for each. Averages were taken for each trial, and percentage error was calculated between all trials.

3.2.3 Cellular Staining and Microscopy

SH-SY5Y nuclei were stained by adding Hoechst 33342 dye (Molecular Probes) to a 10 μM final concentration to cell media and incubating for 10 minutes. Mitochondria were stained by adding Mitotracker dye (Molecular Probes) to a 100 nM final

Reproduced with permission of the copyright owner. Further reproduction prohibited without permission.

concentration to the cell media. Phosphatidylserine in the cell membrane was stained by adding 1.5 μl of Annexin V 594 (Molecular Probes) per 3 ml of annexin-binding buffer (10 mM HEPES, 140 mM NaCl, 2.5 mM $CaCl_2$, pH 7.4), and incubating for 15 minutes. Following incubation of the Hoechst and Mitotracker dyes, the media was removed and replaced with 1X Phosphate Buffered Saline (PBS) pH 7.4. The cells were examined under a fluorescent and phase contrast microscope. Photos were taken at 100, 400, and 600 x magnification and processed using Adobe Photoshop 6.0 software.

3.2.4 Reduced Glutathione (GSH) Measurements

Control and transfected SH-SY5Y cells were treated with 100 μM H_2O_2. Three hours following treatment, the total cell lysate was prepared, and 50 μl of the lysate was added to 100 μl of reaction buffer (1 mM NADPH, 100 mM Na_2HPO_4, 100 units GSH reductase, and 1 mM DTNB). This mixture was incubated for five minutes at room temperature (Baker *et al.*, 1990). Absorbance was measured at 412 nm in a 96-well microtiter plate using Bio-tek EL_x 808ru Ultra Microplate reader. The amount of reduced glutathione was expressed per microgram of measured protein. Three sets of experiments were done and three sets of measurements were taken for each experiment. Averages were calculated from the results in each trial, and the percentage error between each set of experiments was calculated.

3.2.5 Measurement of Total Reactive Oxygen Species (ROS)

Detection of ROS production was monitered using the membrane permeable dye 2',7'-dichlorofluorescein diacetate (DCFDA) (Siraki *et al.*, 2002). Measurement of total ROS production was measured after 3 hours of treatment with 100 μM H_2O_2 in control and transfected SH-SY5Y cells. DCFDA was added to the cell media to a final concentration of 10 μM, and incubated for 10 minutes at 37°C. Cell lysate was collected, and the pellet was resuspended in 1 X PBS, pH 7.4. Fluorescence was measured using a Spectra Max Gemini XS multi-well plate fluorescence reader at

Reproduced with permission of the copyright owner. Further reproduction prohibited without permission.

an excitation wavelenth of 500 nm, and an emission wavelength of 520 nm. Protein estimation was measured using the Bradford reagent at an absorbance of 595 nm. Results were expressed as a measurement of fluorescence units per microgram of protein. Three sets of experiments were done and three sets of measurements were taken for each experiment. Averages were calculated from the results in each trial, and the percentage error between each set of experiments were calculated.

Reproduced with permission of the copyright owner. Further reproduction prohibited without permission.

3.3 Results

3.3.1 Oxidative and Hypoxia Measurements in Undifferentiated SH-SY5Y Cells

Control cells and stable lines of undifferentiated SH-SY5Y cells expressing both GFP and PDI:GFP were subjected to treatment with 100 μM H_2O_2, for one hour. Following three hours, the cells were stained with Hoechst (to examine nuclear morphology) and Mitotracker (to examine mitochondrial membrane potential) dyes to access the morphological characteristics of apoptosis (figure 3.1). Cells were examined under a fluorescent microscope at a magnification of 400 x. For both lines of control cells, the characteristic of nuclear condensation (blue cells) was shown in figure 3.1B and 3.1E by the rounding up, and clumping of cells. Figure 3.1H contains the PDI:GFP cells, showing a reduction in nuclear condensation and cell clumping. The arrow indicates the single apoptotic nucleus found in that frame. A loss of mitochondrial membrane potential of both lines of control cells was observed through the diffusion of the red stain in figure 3.1C and 3.1F. In figure 3.1I containing the PDI:GFP cell line, the presence of more pronounced, stained mitochondria indicates the maintenance of membrane potential. Maintenance of mitochondrial membrane potential was observed in greater than 75% of the observed PDI:GFP containing cells.

Following cellular staining, the total cell lysate of each cell line was collected, and DCFDA, a fluorescent probe which measures the amount of ROS, was added to the lysate. A measurement of the total fluorescence expressed per microgram of protein was quantified (figure 3.2). These experiments were repeated three times, and measurements were taken three times for each trial. Green columns represent ROS measurements in untreated cells, and violet columns represent ROS measurements cells exposed to oxidative stress. In the PDI:GFP cells, there is a reduced production of ROS as compared to the control lines. On average ROS levels increase by 16 fluorescence units per microgram protein in the control cells, whereas they increased only by 5 fluorescence units per microgram protein in the PDI:GFP cells. In parallel,

Reproduced with permission of the copyright owner. Further reproduction prohibited without permission.

the number of micromoles of reduced glutathione produced per microgram of protein was measured in treated and untreated cells. Detection with DTNB determined the number of reduced thiols for undifferentiated cells treated with H_2O_2. Three separate experiments were done measuring the number of reduced thiols, and three measurements were taken for each trial. Green panels in figure 3.3 represent the glutathione measurements in untreated cells, and violet panels represent glutathione measurements in cells exposed to oxidative stress. Figure 3.3 demonstrates a large reduction in the amount of GSH, an average of 2.5 pmol/μg of protein, in both control lines after exposure to oxidative stress. There is a smaller reduction in GSH levels of 0.4 pmol/μg of protein in cells expressing PDI:GFP.

Undifferentiated transiently transfected GFP and PDI:GFP cells were treated with 100 μM H_2O_2, for one hour. Following three hours, the cells were stained with Annexin V dye to observe membrane flipping of phosphatidylserine, which is indicative of the early stages of apoptosis. Once the dye is bound to phosphatidylserine on the outer leaflet, a visible orange colour outling the membrane is present. Cells were examined under a fluorescent microscope at a magnification of 400 x. In figure 3.4A, cells are untreated and there are no GFP expressing cells, and no cells that take up the annexin V dye. In figure 3.4D and 3.4G, untreated cells show the presence of GFP, and PDI:GFP cells, respectively. In both D and G panels, no annexin binding is present as expected in untreated cells. In the transiently transfected GFP cells, figure 3.4E shows only the annexin V binding dye, and figure 3.4F shows the identical field of view with GFP expressing cells. It is observed that the GFP only cells take up the annexin V binding dye indicating phosphatidylserine membrane flipping. In the transiently transfected PDI:GFP cells, figure 3.4H show cells that take up the annexin V binding dye. In figure 3.4I, the identical field of view shows the presence of PDI:GFP expressing cells that did not take up the annexin V stain. Hence, SH-SY5Y cells containing PDI:GFP seem to evade early apoptotic cellular reponses during hypoxic stress.

Undifferentiated control and stably transfected lines of SH-SY5Y were subjected to hypoxic stress for six hours in a hypoxia chamber. All three cell lines were counted in

Reproduced with permission of the copyright owner. Further reproduction prohibited without permission.

three different fields of view, at 0, 4, 6, 12, 24, and 48 hours following treatment. After 48 hours, all control lines were non-viable, whereas the PDI:GFP cell line still had approximately 20% of viable cells (figure 3.5). Therefore, the presence of PDI:GFP in SH-SY5Y cells delays apoptosis caused by hypoxic stress.

3.3.2 Inducing Oxidative Stress in Differentiated SH-SY5Y Cells

Control SH-SY5Y cells, and a stable line of PDI:GFP cells were differentiated over 14 days. Figures 3.6A and 3.6B show phase contrast pictures of the morphology of differentiated control cells before treatment with hydrogen peroxide. The elongation of the cell body, and the neurite growth can be seen between the cells. Figure 3.7 shows the side by side comparison of phase contrast and fluorescence micrscopy pictures of differentiated PDI:GFP cells before treatment with hydrogen peroxide. Cell body elongation, and neurite growth can be seen in the PDI:GFP cells, with the presence of the recombinant PDI:GFP throughout.

Following differentiation, cells were treated with 100 muM H_2O_2, for one hour. After three hours cells were stained with Hoechst and Mitotracker dyes to examine the cells for the apoptotic features of nuclear condensation and mitochondrial membrane potential. Cells were examined under phase contrast and fluorescent microscopy at 400 x magnification. Figures 3.8 and 3.9 are two examples of the comparison of treated control and PDI:GFP cells. All of the nuclei of the control cells were condensed and rounded, indicative of nuclear condensation during cell death in figures 3.8E and 3.9E, whereas most of the nuclei in PDI:GFP cells maintained normal morphology as indicated by the absence of cell rounding, and clumping (figure 3.8F and 3.9F). The blurry red colour seen in figures 3.8C and 3.9C of the control cells indicate a loss of mitochondrial membrane potential. The mitochondrial membrane potential of most PDI:GFP cells remained intact as exhibited by the defined red colour in figures 3.8D and 3.9D. Figure 3.10 shows more phase contrast and fluorescent microscopy pictures of additional PDI:GFP cells after treatment; figures 3.10B and 3.10 D show that

Reproduced with permission of the copyright owner. Further reproduction prohibited without permission.

nuclear morphology is intact, figures 3.10B and 3.10D indicate that mitochondrial membrane potential is preserved. These photographs further support that the presence of PDI:GFP in differentiated SH-SY5Y cells protects against apoptosis induced by oxidative stress.

Reproduced with permission of the copyright owner. Further reproduction prohibited without permission.

3.4 Discussion

Many studies of apoptosis often work towards application for neurodegenerative diseases and stroke. To gather further evidence for PDI as a neuroprotective protein, SH-SY5Y neuroblastoma cells were chosen as an appropriate model. In working with these cells, difficulties arose in that their number of divisions was very limited and finite. It was important to generate lines of stable cells, and perform experiments before cells reached senescence, which usually occurred between divisions 10 and 11. Also, because of this obstacle for every set of experiments undertaken, new stable cell lines had to be generated, and no stocks of cells could be made. This created a quandary in that the characteristics of each new cell line generated may have varied. Characteristics aside, the assumption was made that PDI function within the cell should remain the same.

3.4.1 Stable SH-SY5Y Cells Expressing PDI:GFP are Protective Against Oxidative Stress

Reactive oxygen species in the cell include superoxide, peroxynitrite, and the hydroxy radical. Oxidative stress has been shown to induce apoptosis in systems such as muscle and neuronal cells (Kroemer *et al.*, 1997). Oxidative stress was induced artificially in the cells with hydrogen peroxide treatment. Although not understood, cell death by ROS has been hypothesized to lead to mitochondrial dysfunction with the release of cytochrome C and apoptosis initiating factor, which then activates a caspase pathway (Strasser *et al.*, 2000). Alternatively, ROS could cause DNA damage, and lead to a p53/Bax pathway inducing apoptosis (Li *et al.*, 1999). A recent paper by Chun and coworkers in 2001, proposed that ROS induced JNK1/2-MAPK, followed by cJun phosphorylation, and the expression of cell death genes. If ROS induces cell stress through the JNK1/2-MAPK pathway, then expression of the CMV IE promoter may have been upregulated, and in doing so, upregulated the expression of the recombinant PDI:GFP. This appears to be evident in the results, in that inducing stress with ROS preserved nuclear morphology and mitochondrial membrane

Reproduced with permission of the copyright owner. Further reproduction prohibited without permission.

potential in those cells containing PDI:GFP, whereas cell death was marked in untransfected cells, and transfected cells expressing GFP only. Measurement of ROS produced by the cells after oxidative stress was measured, and showed an average increase of 15 fluorescence units per microgram of protein in both lines of control cells, whereas the average increase in cells expressing the PDI:GFP protein was only 6 fluorescence units per microgram of protein, almost a 3-fold decrease. Clearly, introducing an excess of PDI into SH-SY5Y cells shows to delay the apoptotic mechanism in evading cell death. Phosphatidylserine flipping, an early apoptotic event was detected using Annexin V dye on transiently transfected cells. Annexin V only binds to phosphatidylserine exposed on the cell surface when it flips from the inner to outer leaflet of the cytoplasmic membrane.

3.4.2 Stable SH-SY5Y Cells Expressing PDI:GFP Maintain the Redox Balance

Redox balance throughout the cell is maintained by the relative concentrations of GSH:GSSG. The cytoplasm of the cell is generally a very reducing environment, with concentrations of GSH:GSSG residing around 30:1 - 100:1 (Raina and Missiakas, 1997). Under oxidative stress, the environment in the cytoplasm becomes more oxidative and the concentration of GSH decreases, as it is oxidized to GSSG. GSH levels were measured using 5,5'-dithio-*bis*- (2-nitrobenzoic acid), or DTNB which reacts with free sulfydryl groups resulting in the formation of 2-nitro-5-thiobenzoic acid (TNB) and a mixed disulfide (Riener *et al.*, 2002). The average decrease in GSH levels in both lines of control cells under oxidative stress was 2.5 picomoles per microgram of protein, whereas the average decrease in cells expressing PDI:GFP was only 0.4 picomoles per microgram of protein. This demonstrates that PDI works to maintain the reducing environment within the cells under stress.

Reproduced with permission of the copyright owner. Further reproduction prohibited without permission.

3.4.3 Stable SH-SY5Y Cells Expressing PDI:GFP Delay Apoptosis

Ischemia, a condition caused by lack of oxygen to cells can result in massive cell death, especially in brain stroke. It has been demonstrated that PDI expression is elevated only in the cerebral cortex of rats with brain ischemia, but not in the hippocampus, cerebellum, or other areas (Tanaka *et al.*, 2000). The number of viable cells remaining in control lines and PDI:GFP lines were assessed over a 48 hour period after ischemic stress. By 48 hours all of the control cells had died, whereas the PDI:GFP cell line still had an average of 20% of viable cells remaining. This observation again exhibits the neuroprotective effect PDI has in SH-SY5Y cells.

3.4.4 Differentiated Stable SH-SY5Y Cells Expressing PDI:GFP Protect Cells from ROS

Control and stable cell lines were differentiated not only to localize PDI:GFP within SH-SY5Y cells, but also to examine the presence of nuclear morphology and mitochondrial membrane potential associated with apoptosis following hydrogen peroxide treatment. Over the course of 14 days of treatment and cell differentiation, many cells died in all lines; the stable GFP cell lines did not remain viable, and most had died off by the tenth day. A possible reason for the complication could be the presence of G418 in the serum deprived media containing only BDNF. G418 is a selective antibiotic which can only be metabolized by the enzyme neomycin phosphotransferase, whose gene is found in the pEGFP-N1 plasmid. The presence of G418 in the media keeps the plasmid inside the SH-SY5Y cells. Any cells that do not contain the plasmid, are killed by the toxic antibiotic, as they do not contain the gene to metabolize it. The high copy number of the plasmid also allowed for a high number of plasmid replication. Excess PDI in the PDI:GFP strain may have contributed to the maintenance of the cell line during differentiation. Pictures comparing the control and PDI:GFP line after differentiation show a decreased level of neurite growth in the PDI:GFP line, and a decreased number of neurite contacts made, as compared to

Reproduced with permission of the copyright owner. Further reproduction prohibited without permission.

the control cells. Again, this may be due to the presence of G418 within the media, which may somehow hinder the growth and formation of differentiated cells. Upon treating the cells with hydrogen peroxide, these studies demonstrate definitively that the PDI:GFP cell line does protect the cells from oxidative stress to an extent. Cell death appears to be slowed down in the PDI:GFP cells as compared to the control cells, although initial characteristics of apoptosis begin to appear with the beading of neurites as illustrated in figures 3.8F and 3.9F.

In summary, additional evidence was gathered to support that PDI works as a neuroprotective protein in response to oxidative and ischemic stress. PDI:GFP cells maintained nuclear morphology, and mitochondrial membrane potential during oxidative stress. These cells showed a much lesser increase in the level of ROS produced as compared to the control cells. Reduced glutathione levels in the PDI:GFP cells were closer to untreated levels after oxidative stress than the control cell lines. These effects may be contributed to the upregulation of another protein - ubiquilin, which has been shown to associated with PDI during stress induced cell death (Ko *et al.*, 2002). A marked reduction in the apoptosis of PDI:GFP cells may also be attributed to its anti-chaperone activity within the cell (Quan *et al.*, 1995, Goldberg *et al.*, 1991, Walker and Gilbert, 1997). PDI can act as an anti-chaperone to aggregate unfolded proteins within the endoplasmic reticulum to help protect them from protein degration.

Previous studies have also proposed that ROS may be involved with the activation of NF-κB (Li *et al.*, 1999). A recent study proposed that PDI suppresses NF-κB activity (Higuchi *et al.*, 2004). This may also in some way contribute to cell death protection. This localization of SH-SY5Y cells using recombinant PDI:GFP demonstrated that this protein was found throughout SH-SY5Y cells. Lahav and coworkers (2000) identified PDI at the cell surface of blood platelets mediating integrin-dependent adhesion, although it was not stated how many disulfide bonds are oxidized or reduced in the integrins. During apoptosis, cells begin to detach from each other and from their matrix. The ability of PDI to delay cell death may also be dependent on its ability to promote disulfide exchange in integrin adhesion.

Reproduced with permission of the copyright owner. Further reproduction prohibited without permission.

More research needs to be conducted on the ability of PDI to protect cells from death. Its protein-protein interactions, downstream signalling, and mechanism by which it functions still needs to be elucidated. Once more is understood about PDI, drugs that could further upregulate its expression may be useful in treating stroke victims and other diseases marked by massive cell death.

Reproduced with permission of the copyright owner. Further reproduction prohibited without permission.

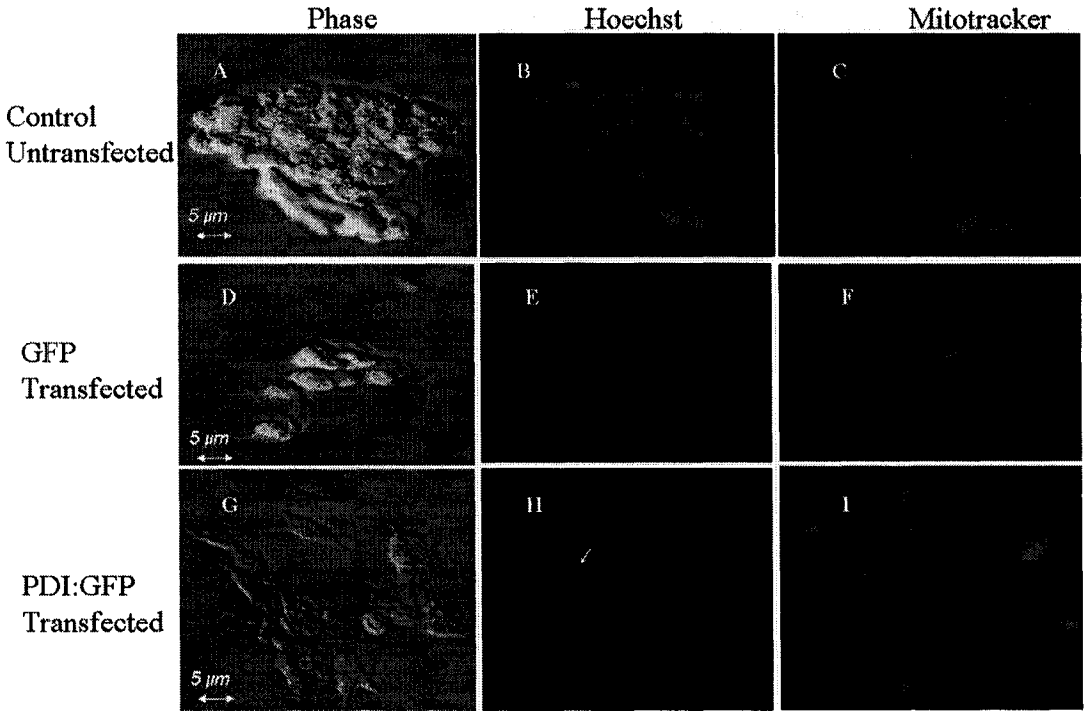

Figure 3.1: Morphology of control and stable SH-SY5Y cells following oxidative stress. Undifferentiated SH-SY5Y cells were treated with 100 μM hydrogen peroxide. Following three hours, cells were examined for the presence of morphological features of apoptosis including cell lifting, nuclear condensation, and mitochondrial membrane potential. Frames A, B, and C show the phase contrast, Hoechst stain, and Mitotracker stain respectively, of the untransfected control cells. Frames D, E, and F show the phase contrast, Hoechst stain, and Mitotracker stain of the GFP transfected control cells. Frames G, H, and I show the phase contrast, Hoechst stain, and Mitotracker stain of the PDI:GFP transfected cells. The arrow in Frame H points to a condensed nucleus found within the PDI:GFP field of view. All photographs were taken at 400 x magnification.

Reproduced with permission of the copyright owner. Further reproduction prohibited without permission.

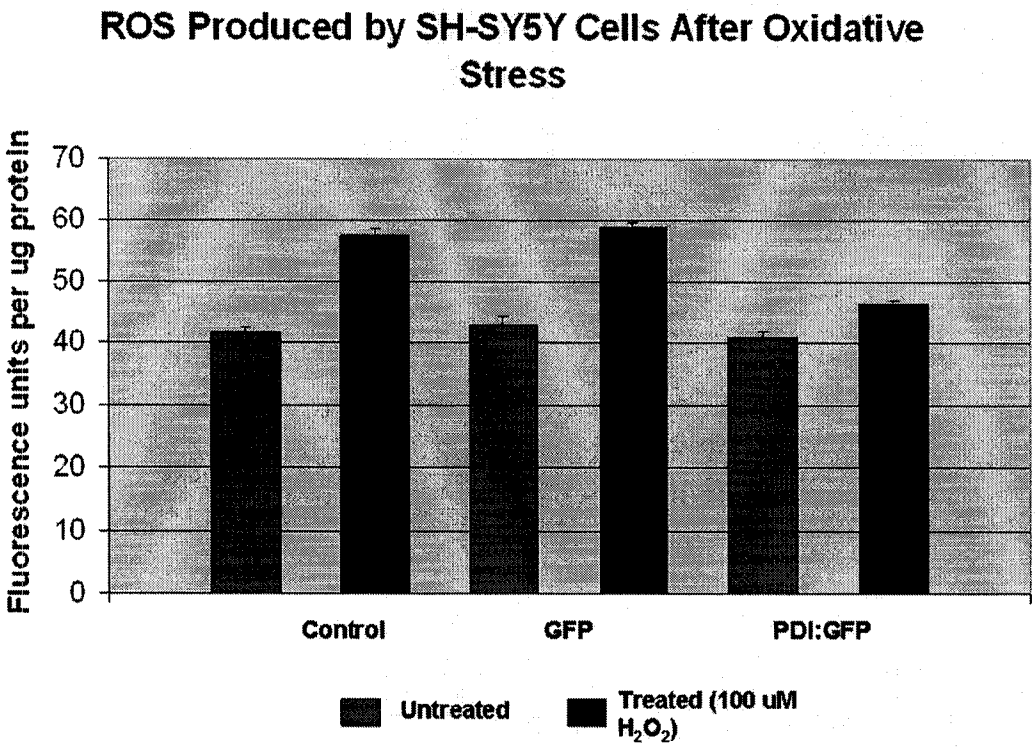

Figure 3.2: Production of reactive oxygen species in control and stable SH-SY5Y cells. Undifferentiated SH-SY5Y cells were treated with 100 μM hydrogen peroxide. After three hours, cell lysate was collected and 2',7'-dihydrofluorescein (DCFDA) fluorescent dye was added to the lysate. Measurements of the reactive oxygen species in both treated and untreated cells were taken, and expressed as the number of fluorescnet units per microgram of protein. The first two bars represent the untransfected control cells, the second set represent the stable cells expressing only GFP, and the third set represent the stable cells expressing PDI:GFP. Error bars are based on the standard error between sets of experiments.

Reproduced with permission of the copyright owner. Further reproduction prohibited without permission.

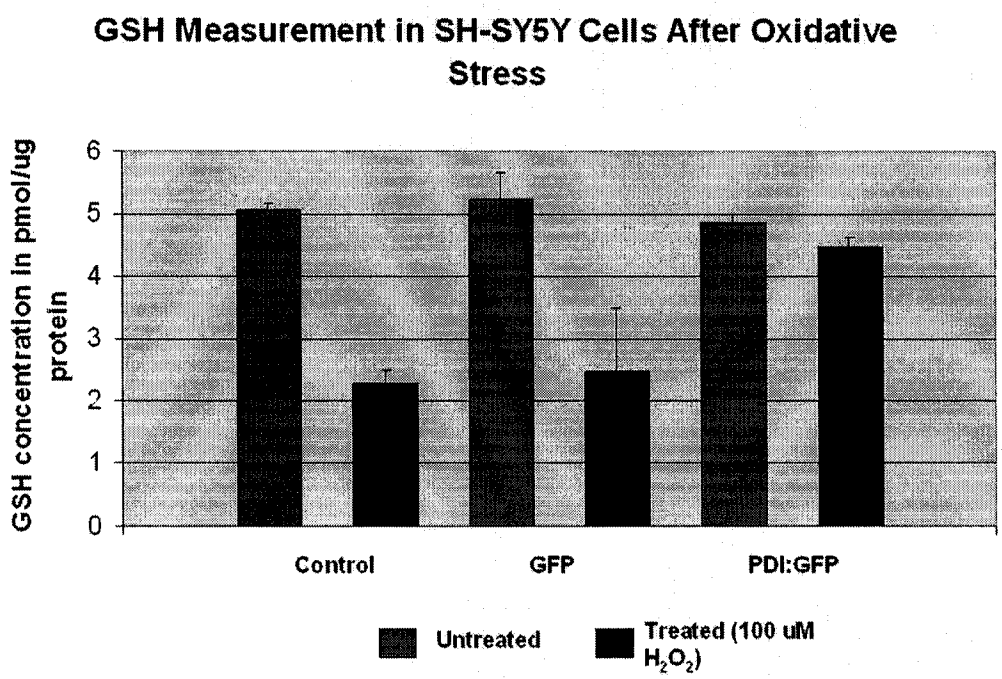

Figure 3.3: Measurement of GSH levels after oxidative stress in control and stable SH-SY5Y cells. Undifferentiated SH-SY5Y cells were treated with 100 μM hydrogen peroxide. Following three hours, cell lysate was collected and incubated with the reaction buffer as described in the methods section. GSH levels in both treated and untreated cells were measured and expressed per microgram of protein. The first two bars represent the untransfected control cells, the second set represents the stable cells expressing only GFP, and the third set represents the stable cells expressing PDI:GFP. Error bars are based on the standard error between sets of experiments.

Reproduced with permission of the copyright owner. Further reproduction prohibited without permission.

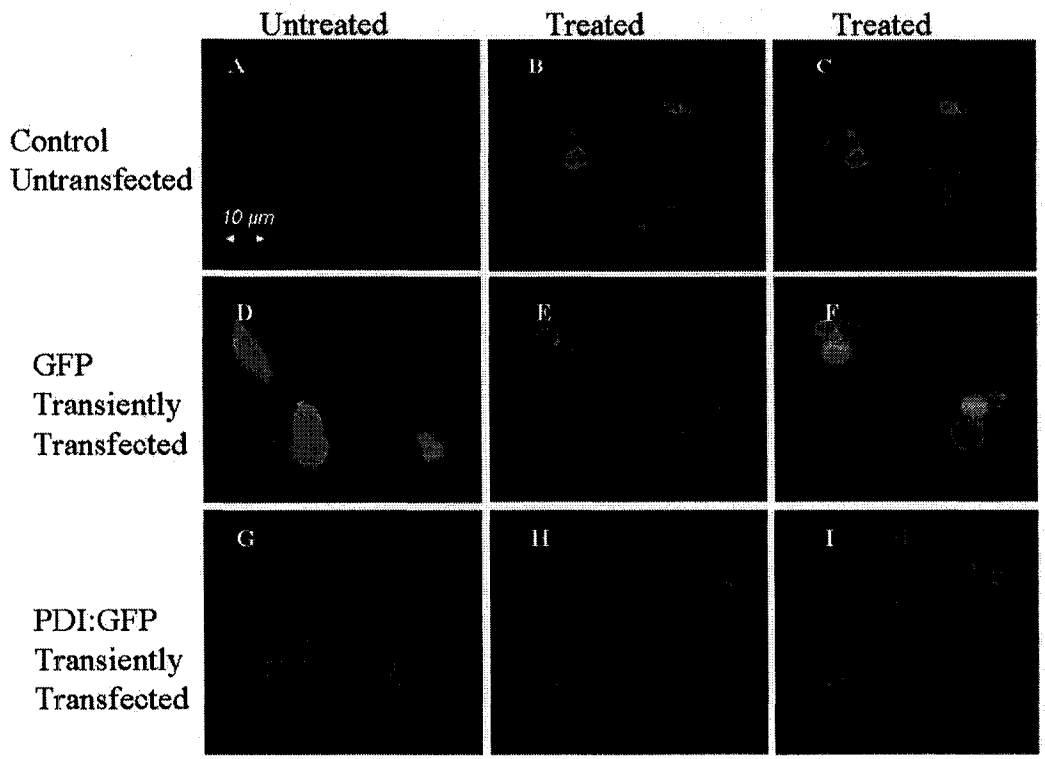

Figure 3.4: Membrane flipping of control and transiently transfected SH-SY5Y cells after oxidative stress. Undifferentiated SH-SY5Y cells were treated with 100 μM hydrogen peroxide. Following three hours, cells were examined for the phosphatidyl serine flipping using Annexin V dye. Frame A shows the untreated control cells, frame B and C show the treated control cells (the same frame is used to show the absence of GFP cells within the control line). Frame D shows untreated GFP cells, frame E displays treated GFP cells, and frame F displays the same field of view as E, but showing both GFP and annexin V binding. Frame G displays untreated PDI:GFP, frame H displays treated PDI:GFP cells, and frame I displays the same field of view as H, but showing both PDI:GFP cells in the presence of annexin V binding. All photographs were taken at 400 x magnification, under fluorescent microscopy.

Reproduced with permission of the copyright owner. Further reproduction prohibited without permission.

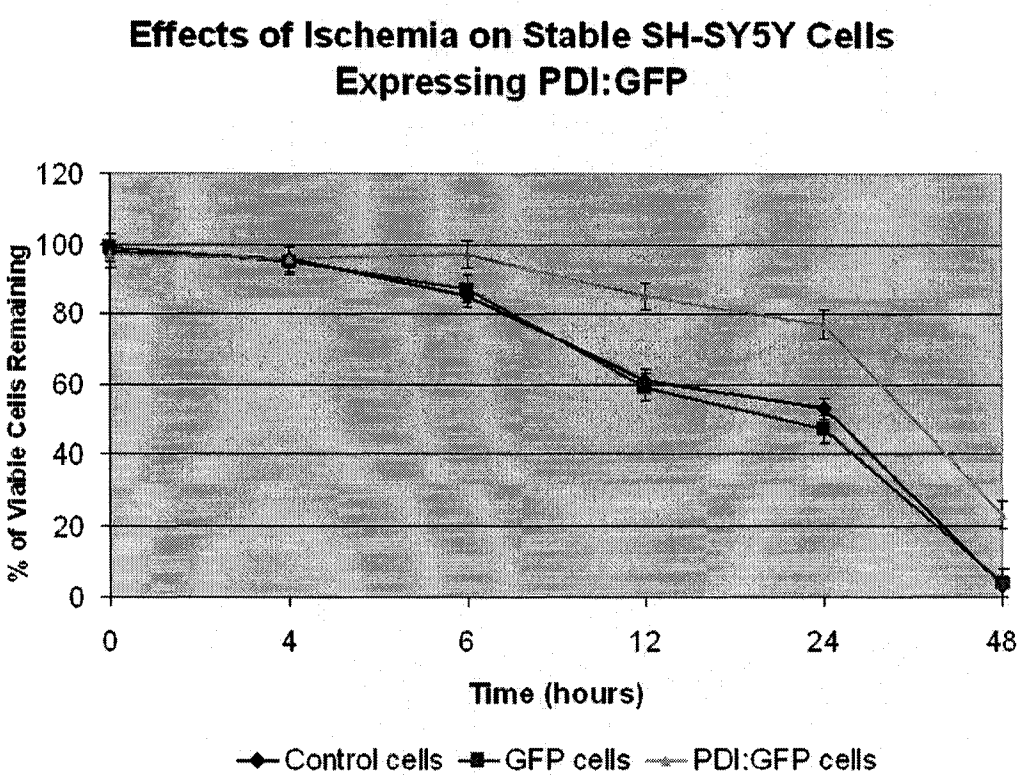

Figure 3.5: Assessment of cell viability following ischemic stress. Undifferentiated control and stable SH-SY5Y lines were subjected to ischemia for 6 hours. Cells were examined using phase contrast microscopy, and three different areas were counted for the number of viable cells following stress induction at time periods of 0, 4, 6, 12, 24, and 48 hours. Results were expressed as a percentage of viable cells remaining. Error bars are based on the standard error between sets of experiments.

Reproduced with permission of the copyright owner. Further reproduction prohibited without permission.

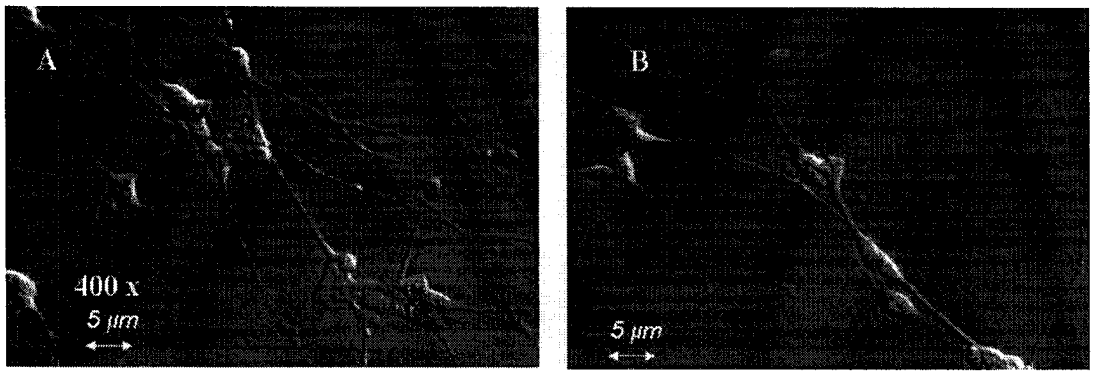

Figure 3.6: Differentiated SH-SY5Y cells before oxidative stress. Cells were differentiated for 14 days as described in the methods section. Phase contrast photographs were taken of the cells prior to inducing oxidative stress, to examine for morphological features of differentiated cells which include, cell body elongation, and neurite lengthening and contact. Frames A and B show two different fields of view of the differentiated control cells. All pictures were taken at 400 x magnification under a phase contrast microscope.

Reproduced with permission of the copyright owner. Further reproduction prohibited without permission.

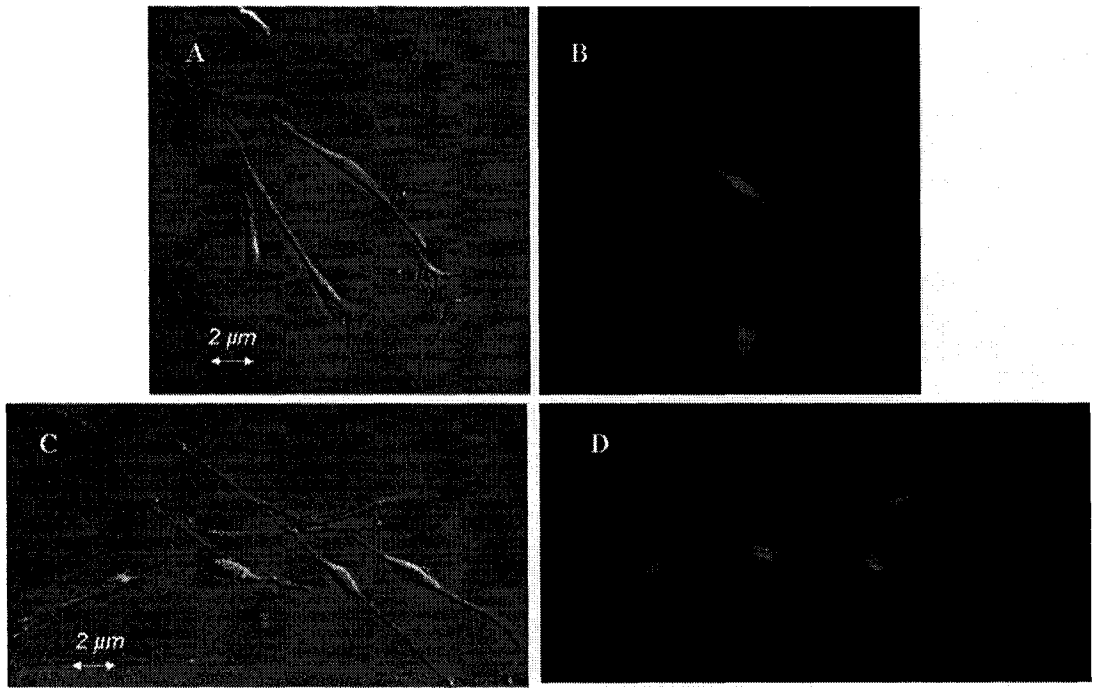

Figure 3.7: Differentiated PDI:GFP SH-SY5Y cells before oxidative stress. Cells were differentiated for 14 days as described in the methods section. Photographs of the cells were taken prior to inducing oxidative stress, to examine morphological features of differentiated cells. Frames A and C show two different fields of view of the differentiated PDI:GFP cells under phase contrast microscopy. Frames B and D show the same frames as A and C, under fluorescent microscopy. Cells in frames B and D were examined for the presence of the recombinant PDI:GFP protein. All pictures were taken at 400 x magnification.

Reproduced with permission of the copyright owner. Further reproduction prohibited without permission.

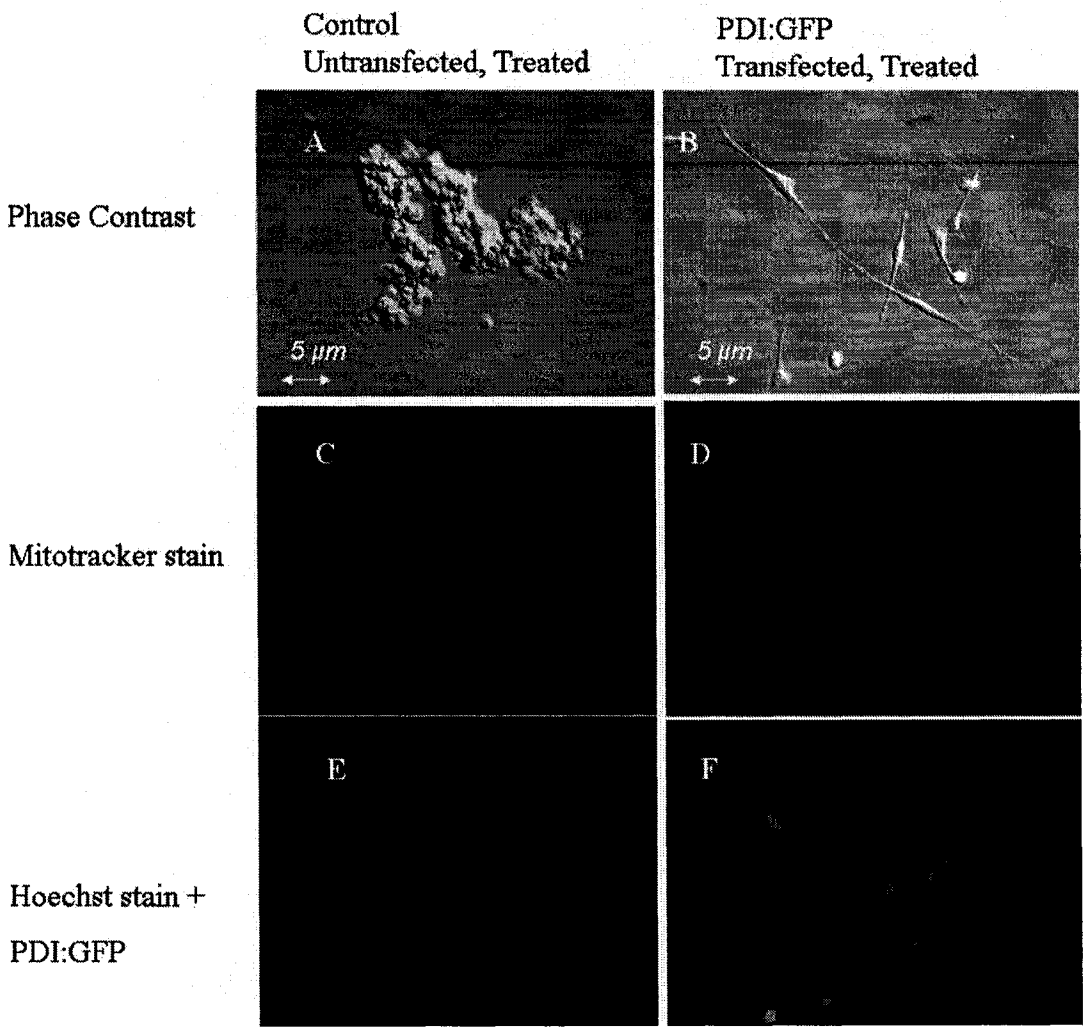

Figure 3.8: Morphology of control and stable differentiated SH-SY5Y cells after oxidative stress. Differentiated SH-SY5Y cells were treated with 100 μM hydrogen peroxide. Following three hours, cells were examined for the presence of the morphological features of apoptosis including cell lifting, nuclear condensation, and mitochondrial membrane potential. Frames A, C, and E show the phase contrast, Hoechst stain, and Mitotracker stain respectively, of the control cells. Frames B, D, and F show the phase contrast, Hoechst stain, and Mitotracker stain of the PDI:GFP cells. All photographs were taken at 400 x magnification. Frames A and B were taken under phase contrast microscopy, and frames C, D, E, and F were taken under fluorescent microscopy.

Reproduced with permission of the copyright owner. Further reproduction prohibited without permission.

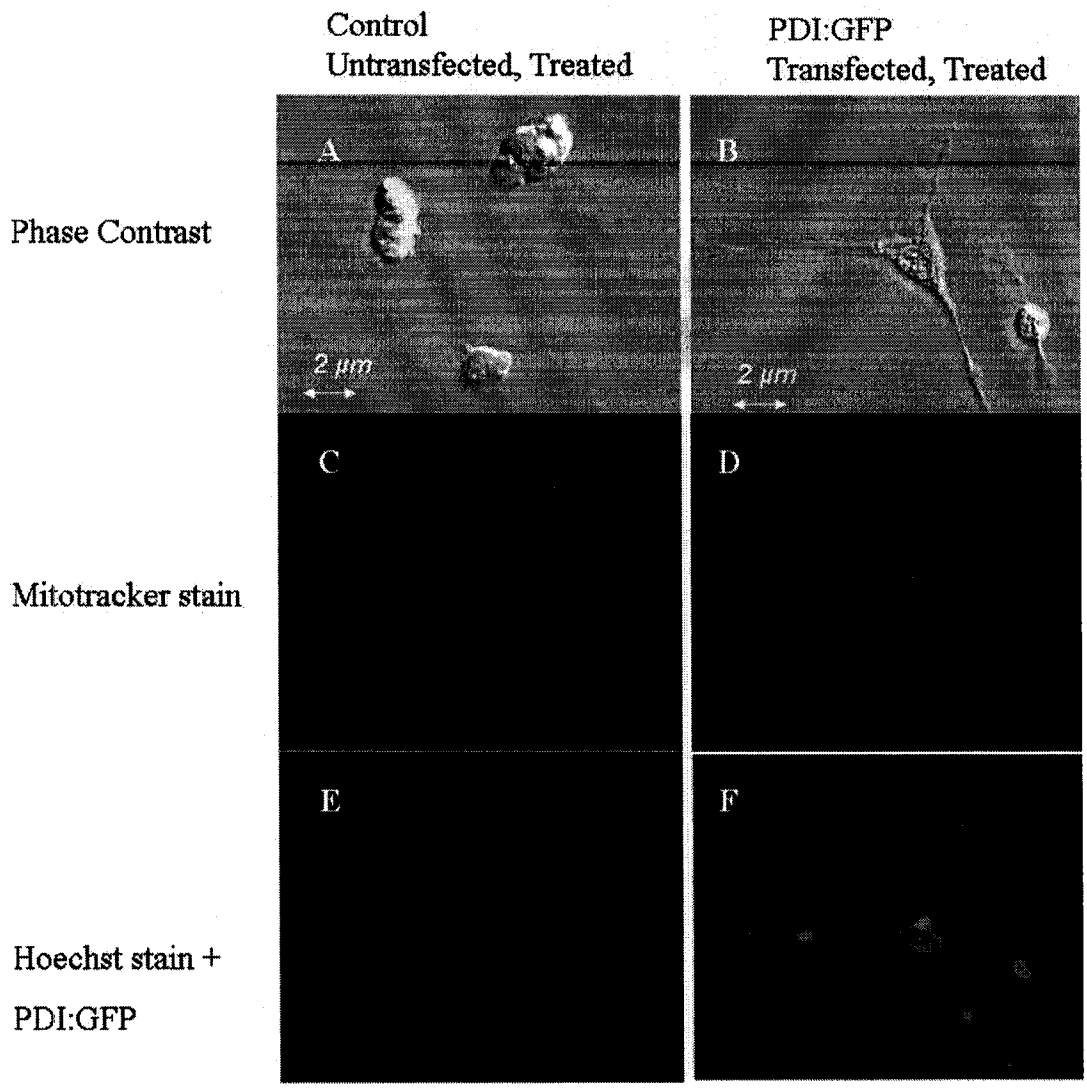

Figure 3.9: Morphology of control and stable differentiated SH-SY5Y cells after oxidative stress. Following three hours, cells were examined for the presence of the morphological features of apoptosis including cell lifting, nuclear condensation, and mitochondrial membrane potential. Frames A, C, and E show the phase contrast, Hoechst stain, and Mitotracker stain respectively, of the control cells. Frames B, D, and F show the phase contrast, Hoechst stain, and Mitotracker stain of the PDI:GFP cells. All photographs were taken at 400 x magnification. Frames A and B were taken under phase contrast microscopy, and frames C, D, E, and F were taken under fluorescent microscopy.

Reproduced with permission of the copyright owner. Further reproduction prohibited without permission.

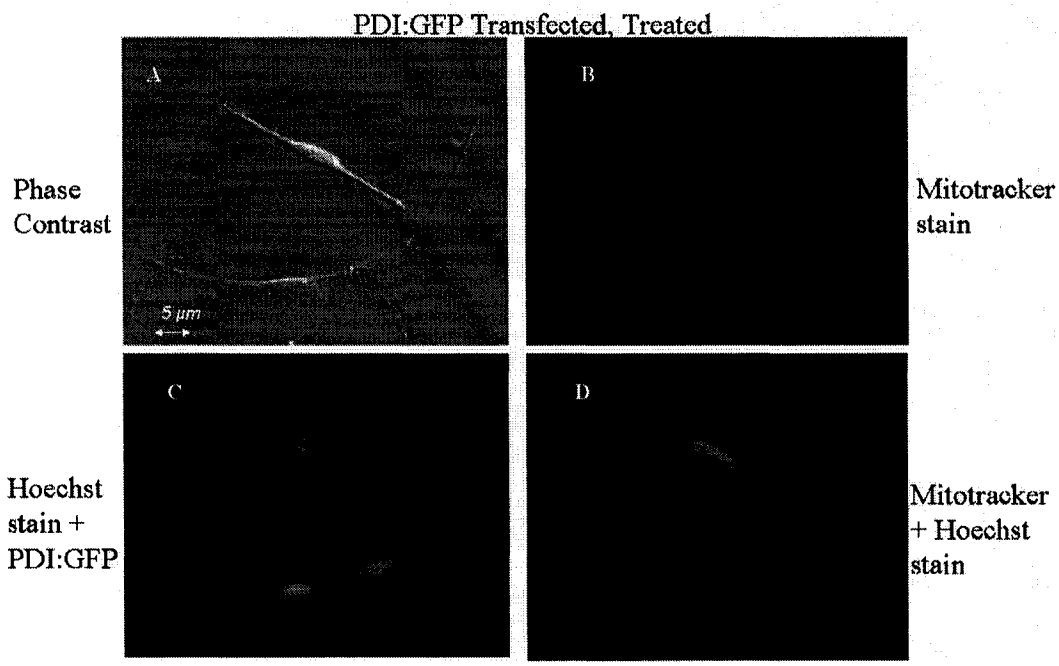

Figure 3.10: Morphology of differentiated PDI:GFP cells following oxidative stress. Differentiated PDI:GFP cells were examined for the presence of the morphological features of apoptosis. Frame A shows cells under phase contrast microscopy, frame B shows cells stained with Mitotracker, frame C shows PDI:GFP protein and Hoechst stained nuclei, and frame D shows cells stained with both Mitotracker and Hoechst. All photographs were taken at 400 x magnification. Frame A was taken under phase contrast microscopy, and frames B, C, and D were taken under fluorescent microscopy.

Reproduced with permission of the copyright owner. Further reproduction prohibited without permission.

Chapter 4

Directions for Future Study

In further studies of PDI as a neuroprotective protein, it is important to determine how it interacts with other molecules within the cell. During ischemic stress, inducible NO synthase is upregulated which generates excess amounts of nitric oxide (Moriya *et al.*, 2000). Moriya and coworkers also demonstrated that excess NO causes apoptosis through the initial loss in mitochondrial membrane potential and final downstream caspase signalling resulting in DNA degradation. It has been suggested that PDI is involved with the transport of intracellular NO equivalents (Sliskovic *et al.*, 2005). Future work could include the study of the addition of PDI:GFP to SH-SY5Y cells, and on the determination of the intracellular NO levels when cells are exposed to ischemic stress. PDI denitrosation activity can easily be monitored with the highly fluorescent and sensitive probe, *N*-dansyl-S-nitrosohomocysteine (DAN), that reacts with NO_x, to form napthotriazole (NAT), which emits a fluorescent signal at 406 nm (Raturi and Mutus, 2004). By using this probe on the cell lysates of PDI:GFP cells exposed to ischemic stress, PDI denitrosation activity can be monitered.

Reproduced with permission of the copyright owner. Further reproduction prohibited without permission.

Literature Cited

Akagi, S., Yamamoto, A., Yoshimori, T., Masaki, R., Ogawa R., and Tashiro, Y. (1988). Localization of protein disulfide isomerase on plasma membranes in rat exocrine pancreatic cells. *J. Histochem. Cytochem.* 36:1069-1074.

Ashkenazi, A. and Dixit, V.M. (1998). Death receptors: signaling and modulation. *Science* 281:1305-1308.

Baker, M.A., Cerniglia, G.J., and Zaman, A. (1990). Microtiter plate assay for the measurement of glutathione and glutathione disulfide in large numbers of biological samples. *Anal. Biochem.* 190(2):360-365.

Berman, H.M., Westbrook, J., Feng, Z., Gilliland, G., Bhat, T.N., Weissig, H., *et al.* (2000). The protein data bank. *Nucleic Acids Research* 28:235-242.

Bernal-Mizrachi, C., Gates, A.C., Weng, S., Imamura, T., Knutsen, R.H., DeSantis, P., Coleman, T., *et al.* (2005). Vascular respiratory uncoupling increases blood pressure and atherosclerosis. *Nature* 435:502-506.

Betteridge D.J. (2000). What is oxidative stress? *Metabolism* 49:3-8.

Bruening, W., Giasson, B., Mushynski, W., and Durham, H.D. (1998). Activation of stress-activated MAP protein kinases up-regulate espression of transgenes driven by the cytomegalovirus immediate/early promoter. *Nucleic Acids Res.* 26:486-489.

Reproduced with permission of the copyright owner. Further reproduction prohibited without permission.

Chen, K., Detwiler, T.C., and Essex, D.V. (1995). Characterization of protein disulphide isomerase released from activated platelets. *British Journal of Haematology* 90:425-431.

Chun, H.S., Gibson, G.E., DeGiorgio, L.A., Zhang, H., Kidd, V.J., and Son, J.H. (2001). Dopaminergic cell death induced by MPP(+), oxidant and specific neurotoxicants shares the common molecular mechanism. *J. Neurochem.* 76:1010-1021.

Corbett, E.F., Oikawa, K., Francois, P., Tessier, D.C., Kay, C., Bergeron, J.J., *et al.* (1999). Ca^{2+} regulation of interactions between endoplasmic reticulum chaperones. *J. Biol. Chem.* 274:6203-6211.

Corder, E.H., Saunders, A.M., Strittmatter, W.J., Schmechel, D.E., Gaskell P.C., Small, G.W., *et al.* (1993). Gene dose of apolipoprotein E type 4 allele and the risk of Alzheimer's disease in late onset families. *Science* 261:921-923.

Dai, Y. and Wang, CC. (1997). A mutant truncated protein disulfide isomerase with no chaperone activity. *J. Biol. Chem.* 272:27572-27576.

Darby, N.J. and Creighton, T.E. (1995). Functional properties of the individual thioredoxin-like domains of protein disulfide isomerase. *Biochemistry* 34:11725-11735.

Darby, N.J. and Creighton, T.E. (1998). The multi-domain structure of protein disulfide isomerase is essential for high catalytic activity. *J. Biol. Chem.* 276:239-247.

Darby, N.J., Kemmink, J. and Creighton, T.E. (1996). Identifying and characterizing a structural domain of protein disulfide isomerase. *Biochemistry*, 35:10517-10528.

Reproduced with permission of the copyright owner. Further reproduction prohibited without permission.

Duke, R.C., Ojcius, D.M., and Young, J.D.E. (1996). Cell suicide in health and disease. *Scientific American*, 12:79-87.

Encinas, M., Iglesias, M., Liu, Y., Wang, H., Muhaisen, A., Cena, *et al.* (2000). Sequential treatment of SH-SY5Y cells with retinoic acid and brain-derived neurotrophic factor gives rise to fully differentiated, neurotrophic factor-dependent, human neuron-like cells. *J. Neurochem.* 75:991-1003.

Essex, D.V. and Li, M. (1999). Protein disulphide isomerase mediates platelet aggregation and secretion. *British Hournal of Haematology* 104:448-454.

Freedman, R.B., Klappa, P., and Ruddock, L.W. (2002). Model peptide substrates and ligands in analysis of action of mammalian protein disulfide-isomerase. *Methods Enzymol.* 348:342-354.

Gibbs, R.A. (1990). DNA amplification by the polymerase chain reaction. *Analytical Chemistry* 62:1202-1214.

Gilbert, H. (1997). Protein disulfide isomerase and assisted protein folding. *J. Biol. Chem.* 272:29399-29402.

Gilbert, H. (1989). Catalysis of thiol/disulfide exchange: single-turnover recution of protein disulfide isomerase by glutathione and catalysis of peptide disulfide reduction. *Biochemistry* 28:7298-7305.

Glasel, J.A. (1995). Validity of nucleic acid purities monitored by A260/A280 absorbance ratios. *Biotechniques*, 18:62-63.

Goldberg, M.E., Rudolph, R., and Jaenicke, R. (1991). A kinetic study of the competition between renaturation and aggregation during the refolding of denatured-

Reproduced with permission of the copyright owner. Further reproduction prohibited without permission.

reduced egg white lysosyme. *Biochemistry* 30:2790-2796.

Goldberger, R.F., Epstein, C.J., and Anfinsen, C.B. (1964). Purification and properties of a microsomal enzyme catalyzing the reactivation of reduced ribonuclease and lysozyme. *J. Biol. Chem.* 239:1406-1410.

Gores, G.J., Herman, B., and Lemasters, J.J. (1990). Plasma membrane bleb formation and rupture: a common feature of hepatocellular injury. *Hepatology* 11:690-698.

Graven, KK., Molvar, C., Roncarati, J.S., Klahn, B.D., Lowrey, S. and Farber, H.W. (2002). Identification of protein disulfide isomerase as an endothelial hypoxic stress protein. *American Journal of Physiol. Lung and Cell Mol. Physiol.* 282:L996-L1003.

Hengartner, M. (2000). The biochemistry of apoptosis. *Nature* 407:770-777.

Higuchi, T., Watanabe, Y., and Waga, I. (2004). Protein disulfide isomerase suppresses the transcriptional activity of NF-κB. *Biochem. Biophys. Res. Comm.* 318:46-52.

Holmgren, A. (1979). Thioredoxin catalyzes the reduction of insulin disulfides by dithiothreitol and dihydrolipoamide. *The Journal of Biological Chemistry* 254:9627-9632.

Horibe, T., Iguchi, D., Masuoka, T., Gomi, M., Kimura, T., and Kikuchi, M. (2004). Replacement of domain b or human protein disulfide isomerase-related protein with domain b' of human protein disulfide isomerase dramatically increases its chaperone activity. *FEBS Lett.* 566:311-315.

Reproduced with permission of the copyright owner. Further reproduction prohibited without permission.

Kamata, H. and Hirata, H. (1999). Redox regulation of cellular signaling. *Cell Signal* 11:1-14.

Kato, K., Rojo, H., Asano, T., and Udaka, J. (1991). Production of human PDI. Patent JP 1991206887-A.

Kerr, J.F.R., Wyllie, A.H., and Currie, A.R. (1972). A basic biological phenomenon with wide ranging implications in tissue kinetics. *British Journal of Cancer* 26:239-257.

Kemmink, J., Darby, N.J., Kijkstra, K., Nilges, M., and Creighton, T.E. (1996). Structure determination of the N-terminal thioredoxin-like domain of protein disulfide isomerase using multidimensional heteronuclear 13C/15N NMR spectroscopy. *Biochemistry* 35:7684-7691.

Kemmink, J., Kijkstra, K., Mariani, M., Scheek, R.M., Penka, E., Nilges, M., Darby, N.J. (1999). The structure in solution of the b domain of protein disulfide isomerase. *J. Biomol. NMR* 13:357-368.

Kim, H.T., Russell, R.L., Raina, A.K., Harris, P.L.R. Siedlak, S.L, Zhu, X., *et al.* (2000). Protein disulfide isomerase in Alzheimer disease. *Antiox. Redox Sign.* 2:485-489.

Klappa, P., Ruddock, L.W., Darby, N., and Freedmann, R.B. (1998). The b' domain provides the principle peptide binding site of protein disulfide isomerase but all domains contribute to binding of misfolded proteins *EMBO J.* 17:927-935.

Ko, H.S., Uerhara, T., and Nomura, Y. (2002). Role of ubiquilin associated with protein-disulfide isomerase in the endoplasmic reticulum in stress-induced apoptotic cell death. *J. Biol. Chem.* 38:35386-35392.

Reproduced with permission of the copyright owner. Further reproduction prohibited without permission.

Koivu, J., Myllyla, R., Helaakoski, T., Pihlajaniemi, T., Tasanen, K., and Kivirikko, K.I. (1987). A single polypeptide acts both as the beta subunit of prolyl 4-hydroxylase and as a protein disulfide-isomerase. *EMBO.* 6:648-649.

Koivunen, P, Pirneskoski, A., Karvonen, P., Ljung, J., Helaakoski, T., Notbohm, H, and Kivirikko, K.I. (1999). The acidic C-terminal domain of protein disulfide isomerase is not critical for the enzyme subunit function or for the chaperone or disulfide activities of the polypeptide. *EMBO J.* 18:65-74.

Kroemer, G., Zamzami, N., and Susin, S.A. (1997). Mitochondrial control of apoptosis. *Immunol. Today* 18:44-51.

Lahav, J., Gofer-Dadosh, N., Luboshitz, J., Hess, O. and Shaklai, M. (2000). Protein disulfide isomerase mediates integrin-dependent adhesion. *FEBS Letters* 475:89-92.

Lebeche, D., Lucero, H.A., and Kaminer, B. (1994). Calcium binding properties of rabbit liver protein disulfide isomerase. *Biochem. Biophys. Res. Commun.* 202:556-561.

Li, P.F., Dietz, R., and von Harsdorf, R. (1999). p53 regulates mitochondrial membrane potential through reactive oxygen species and induces cytochrome c-independent apoptosis blocked by Bcl-2. *EMBO J.* 18:6027-6036.

Lincoln, T.M., Cornwell, L.T., and Taylor, A.E. (1990) cGMP-dependent protein kinase mediates the reduction of Ca^{2+} by cAMP in vascular smooth muscle cells. *Am. J. Physiol.* 258:C399-C407.

Linden, R., Martins, R.A., and Silveira, M.S. (2005). Control of programmed cell

Reproduced with permission of the copyright owner. Further reproduction prohibited without permission.

death by neurotransmitters and neuropeptides in the developing mammalian retina. *Prog. Retin Eye Res.* 4:457-491.

Lu, X., Gilbert, H.F., and Harper, J.W. (1992). Conserved residues flanking the thiol/disulfide centers of protein disulfide isomerase are not essential for catalysis of thiol/disulfide exchange. *Biochemistry* 30:4205-4210.

Lundstrom, J. and Holmgren, A. (1993). Determination of the reduction-oxidation potential of the thioredoxin-like domains of protein disulfide-isomerase from the equilibrium with glutathione and thioredoxin. *Biochemistry* 32:6649-6655.

Lyles, M.M., and Gilbert, H.F. (1991). Catalysis of the oxidative folding of ribonuclease A by protein disulfide isomerase: pre-steady-state kinetics and the utilization of the oxidizing equivalents of the isomerase. *Biochemistry* 30:619-625.

Mah, A., Perry, G., Smith, M.A., and Monterio, M.J. (2000). Identification of ubiquilin, a novel presenilin interactor that increases presenilin protein accumulation. *J. Cell Biol.* 151:847-862.

Marnett, L.J. (2000). Oxyradicals an DNA damage. *Carcinogenesis* 21:361-370.

Moon, Y., Lee, K.H., Park, J.H., Geum, D., and Kim, K. (2005) Mitochondrial membrane depolarization and the selective death of dopaminergic neurons by rotenone: protective effect of coenzyme Q10. *J. Neurochem.* 93:1199-1208.

Moriya, R., Uehara, T, and Nomura, Y. (2000). Mechanism of nitric oxide-induced apoptosis in human neuroblastoma SH-SY5Y cells. *FEBS Letters* 484:253-260.

Morjana, N.A. and Gilbert, H.F. (1991). Catalysis of protein folding by agarose-immobilized protein disulfide isomerase. *Biochemistry* 30:4985-4990.

Reproduced with permission of the copyright owner. Further reproduction prohibited without permission.

Munir, M, Lu, L, and McGonigle, P. (1995). Excitotoxic cell death and delayed rescue in human neurons derived from NT2 cells. *Journal of Neuroscience* 15:7847-7860.

Murzin, A.G., Brenner S.E., Hubbard T., Chothia, C. (1995). SCOP: a structural classification of proteins database for the investigation of sequences and structures. *J. Mol. Biol.* 247:536-540.

Naderi, J., Hung, M., and Pandey, S. (2003). Oxidative stress-induced apoptosis in dividing fibroblasts involves activation of p38 MAP kinase and over-expression of Bax: resistance of quiescent cells to oxidative stress. *Apoptosis* 8:91-100.

Narindrasorasak, S., Yao, P., and Sarkar, B. (2003). Protein disulfide isomerase, a multifunctional protein chaperone, shows copper-binding activity. *Biochem. Biophys. Res. Commun.* 311:405-414.

Nagata, S. (1997). Apoptosis by death factor. *Cell* 88:355-365.

Nagata, S. (2000). Apoptotic DNA fragmentation. *Experimental Cell Research* 256:12-18.

Noiva, R. (1999). Protein disulfide isomerase: the multifunctional redox chaperone of the endoplasmic reticulum. *Semin. Cell. Dev. Biol.* 5:481-493.

Noiva, R., Freedman, R.B., Lennarz, W.J. (1993). Peptide binding to protein disulfide isomerase occurs at a site distinct from the active sites. *J. Biol. Chem.* 268:19210-19217.

Nomura, Y. (2004). Neuronal apoptosis and protection: effects of nitric oxide and

Reproduced with permission of the copyright owner. Further reproduction prohibited without permission.

endoplasmic reticulum-related proteins. *Biol. Pharm. Bull.* 27:961-963.

Pearl, F., Todd, A., Sillitoe, I., Dibley, M., Redfern, O., Lewis, T., *et al.* (2005). The CATH domain structure database and related resources Gene3D and DHS provide comprehensive domain family information for genome analysis. *Nucleic Acids Research* 33:D247-251.

Pollack, M. and Leeuwenburgh, C. (2001). Apoptosis and aging: role of the mitochondria. *J. Ger. Biol. Sci.* 11:B475-B482.

Primm, T.P. and Gilbert, H.F. (2001). Hormone binding by protein disulfide isomerase, a high capacity reservoir of the endoplasmic reticulum. *J. Biol. Chem.* 276(1): 281-286.

Primm, T.D., Walker, K.W., and Gilbert, H.F. (1996). Facilitated protein aggregation. Effects of calcium on the chaperone and anti-chaperone activity of protein disulfide-isomerase. *J. Biol. Chem.* 271:33664-33669.

Puig, A. Lyles, M.M., Noiva, R., and Gilbert, H.F. (1994) The role of the thiol/disulfide centers and peptide binding site in the chaperone and anti-chaperone activity of protein disulfide isomerase. *J. Biol. Chem.* 269:19128-19135.

Quan, H., Fan, G., and Wang, C.C. (1995). Independence of the chaperone activity of protein disulfide isomerase from its thioredoxin-like active site. *J. Biol. Chem.* 270:17078-17080.

Raina, S., and Missiakas, D. (1997). Making and breaking disulfide bonds. *Annu. Rev. Microbiol.* 51:179-202.

Ramachandran, N., Root, P. Jiang, X.M., Hogg, P.J., and Mutus, B. (2001).

Reproduced with permission of the copyright owner. Further reproduction prohibited without permission.

Mechanism of transfer of NO from extracellular S-nitrosothiols into the cytosol by cell-surface protein disulfide isomerase. *PNAS* 98:9539-9544.

Raturi, A. and Mutus, B. (2004). Use of 2,3-diaminonapthalene for studying denitrosation activity of protein disulfide isomerase. *Anal. Biochem.* 326:281-283.

Riener, C.K., Kada, G., and Gruber, H.J. (2002). Quick measurement of protein sulfhydryls with Ellman's reagent and with 4,4'-dithiodipyridine. *Anal. Bioanal. Chem.* 373:266-276.

Rigobello, M.P., Donella-Deana, A.,Cesaro, L., and Bindoli, A. (2000). Isolation, purification, and characterization of a rat liver mitochondrial protein disulfide isomerase. *Free Radical Biology & Medicine* 28:266-272.

Root, P., Sliskovic, I., and Mutus, B. (2004). Platelet cell-surface protein disulphide-isomerase mediated S- nitrosoglutathione consumption. *Biochem. J.* 382:575-580.

Safran, M. and Leonard, J.L. (1991). Characterization of an N-bromoacetyl-L-thyroxine affinity-labeled 55 kilodalton protein as protein disulfide isomerase in cultured glial cells. *Endocrinology* 129:2011-2016.

Sambrook, J., Gritsch, E., and Maniatis, T. (1989). Molecular Cloning: A laboratory manual. Cold Spring Harbor Lab.

Schwaller, M., Wilkinson, B., and Gilbert, H.F. (2003). Reduction-reoxidation cycles contribute to catalysis of disulfide isomerization by protein-disulfide isomerase. *J. Biol. Chem.* 278:7154-7159.

Shin, G.C., Song, M.C., and Scheraga, H.A. (2002). Effect of protein disulfide isomerase on the rate-determining steps of the folding of bovine pancreatic ribonuclease

Reproduced with permission of the copyright owner. Further reproduction prohibited without permission.

A. *FEBS Letters* 521:77-80.

Shoji, Y., Uedono, Y., Ishikura, H., Takeyama, N., and Tanaka, T. (1995). DNA damage induced by tumor necrosis factor- alpha in L929 cells is mediated by mitochondrial oxygen radical formation. *Immunology* 84:543-548.

Siraki, A.G., Pourahmad, J., Chan, T.S., Khon, S., and O'Brien, P.J. (2002). Endogenous and endobiotic reactive oxygen species formation by isolated hepatocytes. *Free Radical Biology & Medicine* 32:2-10.

Sliskovic, I., Raturi, A., and Mutus, B. (2005). Characterization of the S-denitrosation activity of protein disulfide isomerase. *J. Biol. Chem.* 280:8733-8741.

Smith, C.A., Farah, T., and Goodwin, R.G. (1994). The TNF receptor superfamily of cellular and viral proteins: activation, costimulation, and death. *Cell* 76:959-962.

Strasser, A., O'Connor, L., and Dixit, V.M. (2000). Apoptosis signaling. *Annu. Rev. Biochem.* 69:217-245.

Tanaka, S., Uehara, T., and Nomura, Y. (2000). Up-regulation of protein disulfide isomerase in response to hypoxia/brain ischemia and its protective effect against apoptotic cell death. *J. Biol. Chem.* 275:10388-10393.

Tartaglia, L.A., Ayres, T.M., Wong, G.H.W., and Goeddel, D.V. (1993). A novel domain within the 55 kD TNF receptor signals cell death. *Cell* 74:845-853.

Tatton, W.G. and Olanow, C.W. (1999). Apoptosis in neurodegenerative diseases: the role of mitochondria. *Biochimica et Biophysica Acta* 1410:195-213.

Reproduced with permission of the copyright owner. Further reproduction prohibited without permission.

Thornberry, N. and Yuri, L. (1998). Caspases: enemies within. *Science* 281:1312-1316.

Tian, R., Li, S., Wang, D., Zhao, Z., Liu, Y., and He, R. (2004). The acidic C-terminal domain stablilizes the chaperone function of protein disulfide isomerase. *J. Biol. Chem.* 279:48830-48835.

Todd, M.J., Lorimer, G.H., and Thirumalai, D. (1996). Chaperonin-facilitated protein folding: optimization of rate and yield by an iterative annealing mechanism. *Proc. Natl. Acad. Sci.* 93:4030-4035.

Tzen, C-Y., Filipak, M., Scott, R.E. (1990). Metaplastic change in mesenchymal stem cells induced by activated *ras* oncogene. *American Journal of Pathology* 137: 1091 - 1098.

Villa, P., Kaufmann, S.H., and Earnshaw, W.C. (1997). Caspases and caspase inhibitors. *Trends in Biochemical Sciences* 22:388-393.

Walker, K.W. and Gilbert, H.F. (1997). Scanning and escape during protein-disulfide isomerase-assisted protein folding. *J. Biol. Chem.* 272:8845-8848.

Wetterau, J.R., Aggerbeck, L.P., Laplaud, P.M., and McLean, L.R. (1991). Structural properties of the microsomal triglyceride-transfer protein complex. *Biochemistry* 30:4406-4412.

Yoo, B.C., Krapfenbauer, K., Cairns, N, Belay, G., Bajo, M., and Lubec, G. (2002). Overexpressed protein disulfide isomerase in brains of patients with sporadic Creutzfeldt-Jakob disease. *Neuroscience* 334:196-200.

Zai, A., Rudd, A.M., Scribner, A.W., and Loscalzo, J. (1999). Cell-surface protein

Reproduced with permission of the copyright owner. Further reproduction prohibited without permission.

disulfide isomerase catalyzes transnitrosation and regulates intracellular transfer of nitric oxide. *The Journal of Clinical Investigation* 103(3):393-399.

Zhao, T.J., Ou, W.B., Xie, Q., Liu, Y., Yan Y.B., and Zhou, H.M. (2005). Catalysis of creatine kinase refolding by protein disulfide isomerase involved disulfide cross-link and dimer to tetramer switch. *J. Biol. Chem.* 14: 13470-13476.

Reproduced with permission of the copyright owner. Further reproduction prohibited without permission.

Appendix A

The PDI sequence used throughout this thesis was obtained from the PDI cDNA cloned into the pET-11a vector, and sequenced at the Wayne State sequencing facility. Conversion of the DNA to protein sequence was done using the ExPASy proteomic tool from *www.expasy.org*.

```
1                   10                  20
D A P E E E D H V L V L R K S N F A E A L A A H K Y
      30                  40                  50
L L V E F Y A P W C G H C K A L A P E Y A K A A G K
                60                  70
L K A E G S E I R L A K V D A T E E S D L A Q Q Y G V
80                  90                  100
R G Y P T I K F F R N G D T A S P K E Y T A G R E A D
       110                 120                 130
D I V N W L K K R T G P A A T T L P D G A A A E S L
              140                 150                 160
V E S S E V A V I G F F K D V E S D S A K Q F L Q A A
                    170                 180
E A I D D I P F G I T S X S D V F S K Y Q L D K D G V
     190                 200                 210
V L F K K F D E X R N N F E G E V T K G E P A G L Y
              220                 230                 240
Q T Q P A A P C H R V P E Q T A P K I F G G X I K T H
                    250                 260
I L L F L P F L P K S V S D Y D G K L S N F K T A A E S
  270                 280                 290
F K G K I L F I F I D S D H T D N Q R I L E F F G L K K
       300                 310                 320
E E C P A V R L I T L E E E M T K Y K P E S E E L T A
              330                 340                 350
E R I T E F C H R F L E G K I K P H L M S Q E L P E C
                    360                 370
W D K Q P V K V L V G K N F E D V A F D E K K N V F
       380                 390                 400
V E F Y A P W C G H C K Q L A P I W D K L G E T Y K
                410                 420
D H E N I V I A K M D S T A N E V E A V K V H S F P T
430                 440                 450
L K F F P A S A D R T V I D Y N G E R T L D G F K K F
     460                 470                 480
L E S G G Q D G A G D D D D L E D L E E A E E P D M
                490
E E D D D Q K A V K D E L
```


Reproduced with permission of the copyright owner. Further reproduction prohibited without permission.

Appendix B

pET-28b vector from Novagen *www.novagen.com*

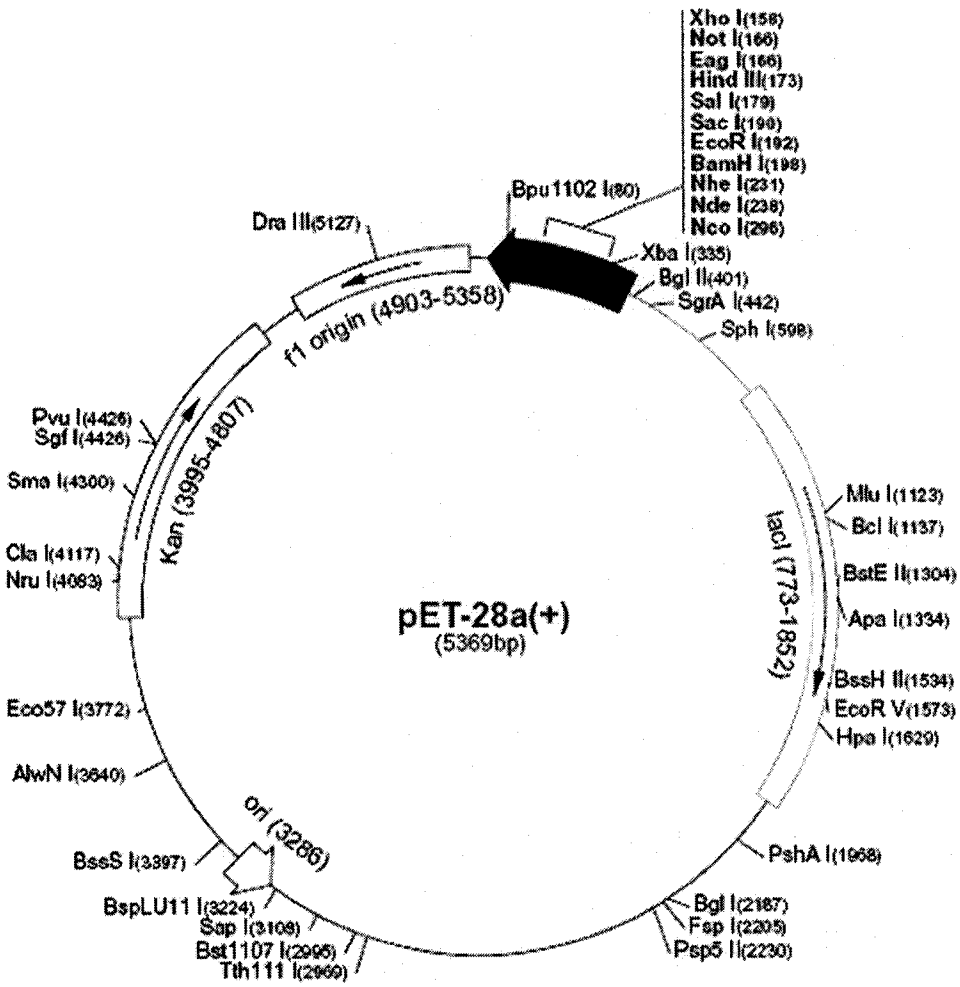

Reproduced with permission of the copyright owner. Further reproduction prohibited without permission.

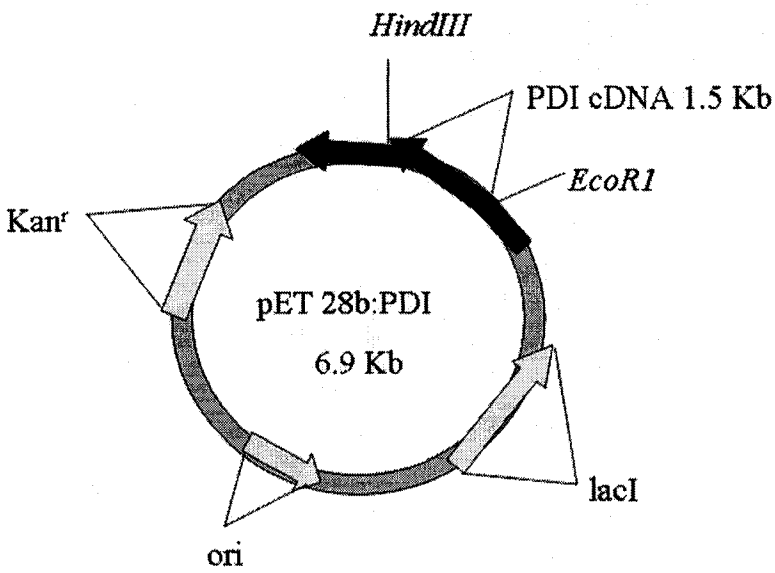

pET-28b:PDI construct

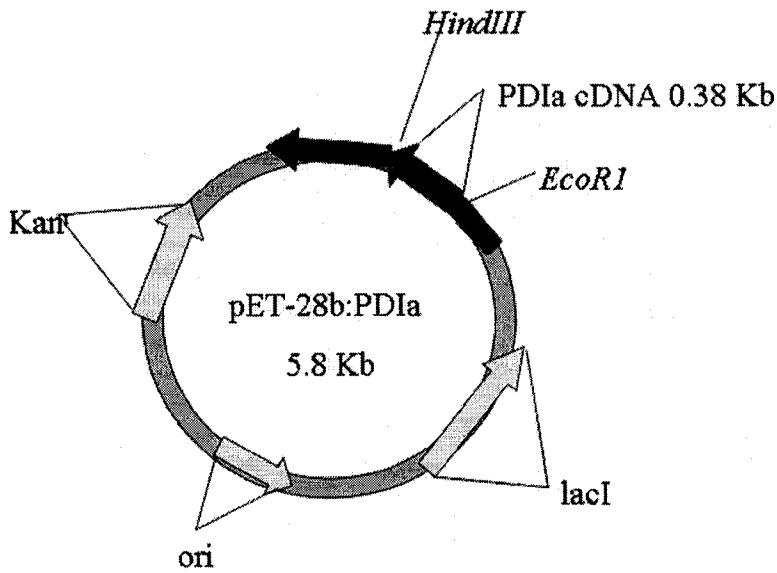

pET-28b:PDIa construct

Reproduced with permission of the copyright owner. Further reproduction prohibited without permission.

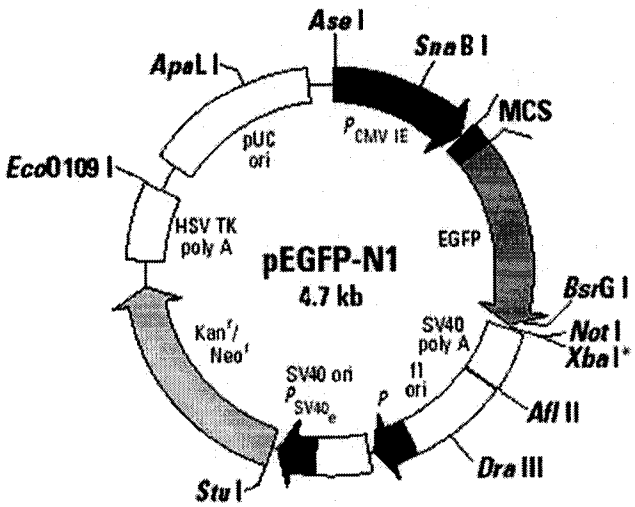

pEGFP-N1 vector from Clontech *www.clontech.com*

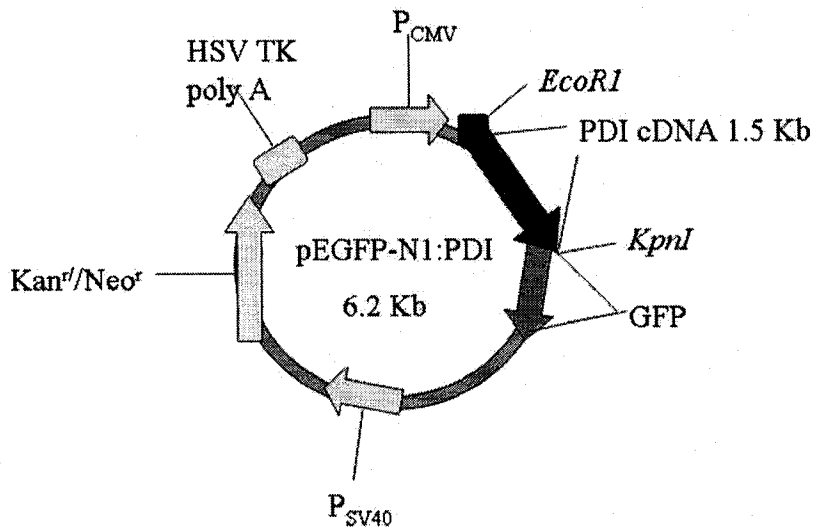

PDI:pEGFP-N1 construct

Reproduced with permission of the copyright owner. Further reproduction prohibited without permission.

Appendix C

Below is the FORTRAN 90 code to generate primers given an insert and vector saved in FASTA format under insert.txt and vector.txt respectively. Once the program is opened, answer the list of questions prompted by the program. Restriction enzymes are to be entered by nucleotide sequence instead of names. Once all of the information has been inputted, the program will generate forward and reverse primers in the 5' to 3' direction based on the information given.

```
PROGRAM primer

INTEGER amax, vmax, cmax, emax
PARAMETER (amax=2500, vmax=500, cmax=100, emax=10)
CHARACTER rdarray*(amax),rdrev*(amax)
CHARACTER insertfor*(cmax), insertmed*(cmax), insertrev*(cmax), &
          vectorfor*(vmax), vectormed*(vmax), vectorrev*(vmax), &
          enza*(emax), enzb*(emax),&
          out1*(cmax),out2*(cmax)
INTEGER a,b,i,j,k,ktot,nrd
INTEGER nc,ng,nt,na,nins,nvec,ntempfor,ntemprev,&
        nenza,nenzb,cut1,cut2,rf1,rf2,&
        pos1,pos2,pos3,nbuff,nout1,nout2,&
        ocut1,ocut2
CHARACTER n*1,choice*1,buff1*1,buff2*1
LOGICAL found
REAL t1,t2,t
REAL temperaturefor(cmax),temperaturerev(cmax)

write(*,*)'****************************************'
write(*,*)'* ------------------------------------ *'
write(*,*)'*|   Primer Generator                  |*'
write(*,*)'*|   By: R.A. Nistor and D. Seslija    |*'
write(*,*)'*|   To be used under the GNU Licence. |*'
write(*,*)'* ------------------------------------ *'
write(*,*)'*|   Comments?  Questions? ... :(      |*'
write(*,*)'* ------------------------------------ *'
write(*,*)'****************************************'

write(*,*)'------------------------------------------'

a=amax
open (unit=80, file='insert.txt', status='OLD' )
read (unit=80,fmt='(A\a)')rdarray
```


Reproduced with permission of the copyright owner. Further reproduction prohibited without permission.

```
call CAPITALIZE(rdarray,amax)
call CHECKARRAY(rdarray,amax)
nins=FINDSIZE(rdarray,amax)
call COUNTNUCS(rdarray,amax,nins,nc,ng,nt,na,ns)
write(*,fmt='(A10,I5,A18)')'Insert is', nins,'nucleotides long.'
write(*,fmt='(A9,I4,A3,I4,A3,I4,A3,I4,A19,I4,A8)')&
          'Contains',nc,'C,',ng,'G,',nt,'T,',&
          na,'A nucleotides, and',ns,'spaces.'
call ASSIGN(rdarray,cmax,insertfor)
call REVASSIGN(rdarray,nins,cmax,insertmed)
call COMPLIMENT(insertmed,cmax,insertrev)
call BLANK(rdarray)
close (unit=80)

write(*,*)'----------------------------------------'

open(unit=81, file='vector.txt', status='OLD' )
read (unit=81,fmt='(A\a)')rdarray

call CAPITALIZE(rdarray,amax)
call CHECKARRAY(rdarray,amax)
nvec=FINDSIZE(rdarray,amax)
call COUNTNUCS(rdarray,amax,nvec,nc,ng,nt,na,ns)
write(*,fmt='(A10,I4,A18)')'Vector is', nvec,' nucleotides long.'
write(*,fmt='(A9,I3,A3,I3,A3,I3,A3,I3,A19,I3,A8)')&
          'Contains',nc,'C,',ng,'G,',nt,'T,',&
          na,'A nucleotides, and',ns,'spaces.'
call ASSIGN(rdarray,vmax,vectorfor)
call REVASSIGN(rdarray,nvec,vmax,vectormed)
call COMPLIMENT(vectormed,vmax,vectorrev)
call BLANK(rdarray)
close (unit=81)

!write(*,*)insertfor(1:cmax)
!write(*,*)insertrev(1:cmax)
!write(*,*)vectorfor(1:nvec)
!write(*,*)vectorrev(1:nvec)
!stop

write(*,*)'----------------------------------------'

100 continue
write(*,*)'Please enter a Temperature range (in Cel.)'
write(*,fmt='(\A10)')' Initial: '
read(*,*)t1
write(*,fmt='(\A10)')'   Final: '
read(*,*)t2
write(*,fmt='(A21,F6.1,A3,F6.1,A10)')'Temperature range = ',&
        t1,'to',t2,' deg. Cel.'
write(*,*)'----------------------------------------'

nc=0; ng=0; nt=0; na=0; ns=0;
found=.false.
do 20 i=1,cmax
  if ( insertfor(i:i).eq.'C' ) nc=nc+1
  if ( insertfor(i:i).eq.'G' ) ng=ng+1
  if ( insertfor(i:i).eq.'T' ) nt=nt+1
  if ( insertfor(i:i).eq.'A' ) na=na+1
  t=TEMP(nc,ng,nt,na)
  temperaturefor(i)=t
  if ( t.ge.t1 .AND. t.le.t2 ) then
    found=.true.
    ntempfor=i
```


Reproduced with permission of the copyright owner. Further reproduction prohibited without permission.

```
    write(*,fmt='(A31,I2,A4,F6.1,A11)')'For insert, found at position ',&
            i,', T=',t
    goto 200
  endif
  if ( .NOT.found .AND. t.gt.t2 ) then
    write(*,*)'ERROR: Temperature range is possibly too small for insert'
    write(*,fmt='(A24,I3,A7,F6.1,A2,F6.1)')'For nucleotide position',&
             i,', T = ',temperaturefor(i-1),'-',t
    write(*,*)'----------------------------------------'
    goto 100
  endif
  if ( i.eq.cmax) then
    write(*,*)'ERROR:  Temperature range too high'
    write(*,fmt='(A18,F6.1)')'Max possible T = ',t
    write(*,*)'----------------------------------------'
    goto 100
  endif
20 continue

200 continue

nc=0; ng=0; nt=0; na=0; ns=0;
found=.false.
do 21 i=1,cmax
  if ( insertrev(i:i).eq.'C' ) nc=nc+1
  if ( insertrev(i:i).eq.'G' ) ng=ng+1
  if ( insertrev(i:i).eq.'T' ) nt=nt+1
  if ( insertrev(i:i).eq.'A' ) na=na+1
  t=TEMP(nc,ng,nt,na)
  temperaturerev(i)=t
  if ( t.ge.t1 .AND. t.le.t2 ) then
    found=.true.
    ntemprev=i
    write(*,fmt='(A42,I2,A4,F6.1,A11)')&
           'For insert compliment, found at position ',i,', T=',t
    goto 300
  endif
  if ( .NOT.found .AND. t.gt.t2 ) then
    write(*,*)'ERROR: Temperature range is possibly too small for insert comp.'
    write(*,fmt='(A24,I3,A7,F6.1,A2,F6.1)')'For nucleotide position',&
             i,', T = ',temperaturerev(i-1),'-',t
    write(*,*)'----------------------------------------'
    goto 100
  endif
  if ( i.eq.cmax) then
    write(*,*)'ERROR:  Temperature range too high'
    write(*,fmt='(A18,F6.1)')'Max possible T = ',t
    write(*,*)'----------------------------------------'
    goto 100
  endif
21 continue

300 continue
a=emax
write(*,*)'----------------------------------------'

write(*,fmt='(\A42)')'Please enter the 1st restriction enzyme: '
read(*,fmt='(A\a)')enza

call CAPITALIZE(enza,emax)
call CHECKARRAY(enza,emax)
nenza=FINDSIZE(enza,emax)
```


Reproduced with permission of the copyright owner. Further reproduction prohibited without permission.

```
write(*,fmt='(\A41)')'After what position is this enzyme cut: '
read(*,*)cut1

write(*,fmt='(\A42)')'Please enter the 2nd restriction enzyme: '
read(*,fmt='(A\a)')enzb

call CAPITALIZE(enzb,emax)
call CHECKARRAY(enzb,emax)
nenzb=FINDSIZE(enzb,emax)

write(*,fmt='(\A41)')'After what position is this enzyme cut: '
read(*,*)cut2

if ( cut1.gt.nenza .OR. cut2.gt.nenzb) then
  write(*,*)'ERROR: cut range beyond the size of the enzyme'
  goto 300
endif

write(*,*)'----------------------------------------'
write(*,fmt='(\A25)')'1st restriction enzyme: '
do 22 i=1,nenza
  write(*,fmt='(\A1)')enza(i:i)
  if ( i.eq.cut1 ) write(*,fmt='(\A1)')'|'
22 continue
write(*,*)
write(*,fmt='(\A25)')'2nd restriction enzyme: '
do 23 i=1,nenzb
  write(*,fmt='(\A1)')enzb(i:i)
  if ( i.eq.cut2 ) write(*,fmt='(\A1)')'|'
23 continue
write(*,*)

400 continue
write(*,fmt='(\A51)')'Are you satisfied with these selections (y or n)? '
read(*,*)choice
if ( choice.eq.'y' ) then
  goto 500
else if ( choice.eq.'n' ) then
  goto 300
else if (choice.ne.'y' .AND. choice.ne.'n') then
  goto 400
endif

500 continue
write(*,*)'----------------------------------------'

pos1=0
pos2=0
call FINDENZ(vectorfor,vmax,nvec,enza,emax,nenza,pos1)
call FINDENZ(vectorfor,vmax,nvec,enzb,emax,nenzb,pos2)
call FINDENZ(vectorrev,vmax,nvec,enzb,emax,nenzb,pos3)

if ( pos1.eq.0 ) then
  write(*,*)'ERROR: 1st restriction enzyme not found in vector'
  goto 300
endif

if ( pos2.eq.0 ) then
  write(*,*)'ERROR: 2nd restriction enzyme not found in vector'
  goto 300
endif

if ( pos1.gt.pos2 ) then
```


Reproduced with permission of the copyright owner. Further reproduction prohibited without permission.

```
  write(*,*)'ERROR: 2nd restriction enzyme found before 1st.'
600 continue
  write(*,fmt='(\A29)')'Enter new enzymes (y or n)? '
  read(*,*)choice
  if ( choice.eq.'y' ) then
    goto 300
  else if ( choice.eq.'n' ) then
    stop
  else if ( choice.ne.'y' .AND. choice.ne.'n' ) then
    goto 600
  endif
endif

write(*,fmt='(A10,A20,I3,A10)')enza(1:nenza),' occurs at position',pos1,&
                               'in vector'
write(*,fmt='(A10,A20,I3,A10)')enzb(1:nenzb),' occurs at position',pos2,&
                               'in vector'
write(*,fmt='(A10,A20,I3,A21)')enzb(1:nenzb),' occurs at position',pos3,&
                               'in vector compliment'
write(*,*)'----------------------------------------'

if ( pos3.eq.0 ) then
  write(*,*)'ERROR: restriction enzyme not found in the compliment.'
  write(*,*)'In the 5p -> 3p directions, the vector and compliment are:'
  write(*,*)vectorfor(1:nvec)
  write(*,*)vectorrev(1:nvec)
  do 28 i=1,nvec
    if ( i-(i/10)*10.eq.0  ) then
      write(*,fmt='(\A)')'|'
    else
      write(*,fmt='(\A)')'.'
    endif
  28 continue
  write(*,*)
  stop
endif

call FINDRF(vectorfor,vmax,nvec,pos1,rf1)
call FINDRF(vectorrev,vmax,nvec,pos3,rf2)

nbuff1=rf1+2
nbuff2=rf2+2

write(*,fmt='(\A57)')'Please enter the 1st buffer nucleotide (c, g, t, or a): '
read(*,*)buff1
call CAPITALIZE(buff1,1)
call CHECKARRAY(buff1,1)
write(*,fmt='(\A57)')'Please enter the 2nd buffer nucleotide (c, g, t, or a): '
read(*,*)buff2
call CAPITALIZE(buff2,1)
call CHECKARRAY(buff2,1)

do 30 j=1,nbuff1
  out1(j:j)=buff1
30 continue
j=nbuff1+1
do 31 i=1,nenza
  if ( enza(i:i).ne.' ' ) then
    if ( i.eq.cut1 ) ocut1=j
    out1(j:j)=enza(i:i)
    j=j+1
  endif
31 continue
```


Reproduced with permission of the copyright owner. Further reproduction prohibited without permission.

```
out1(j:j)='A'
out1(j+1:j+1)='T'
out1(j+2:j+2)='G'
j=j+3
do 32 i=1,ntempfor
  if ( insertfor(i:i).ne.' ' ) then
    out1(j:j)=insertfor(i:i)
    j=j+1
  endif
32 continue
nout1=FINDSIZE(out1,cmax)

do 33 j=1,nbuff2
  out2(j:j)=buff2
33 continue
j=nbuff2+1
do 34 i=1,nenzb
  if ( enzb(i:i).ne.' ' ) then
    if ( i.eq.cut2 ) ocut2=j
    out2(j:j)=enzb(i:i)
    j=j+1
  endif
34 continue
do 35 i=1,ntemprev
  if ( insertrev(i:i).ne.' ' ) then
    out2(j:j)=insertrev(i:i)
    j=j+1
  endif
35 continue
nout2=FINDSIZE(out2,cmax)

write(*,*)'-----------------------------------------'
write(*,*)'Primers in the 5p -> 3p direction are:'
write(*,*)
write(*,fmt='(A18,F6.1,\A3)')'Forward Primer (T=',temperaturefor(ntempfor),'): '
do 40 i=1,nout1
  write(*,fmt='(\A1)')out1(i:i)
  if ( i.eq.ocut1 ) write(*,fmt='(\A1)')'|'
  if ( i-(i/3)*3.eq.0 ) write(*,fmt='(\A1)')' '
40 continue
write(*,*)
write(*,fmt='(A18,F6.1,\A3)')'Reverse Primer (T=',temperaturerev(ntemprev),'): '
do 41 i=1,nout2
  write(*,fmt='(\A1)')out2(i:i)
  if ( i.eq.ocut2 ) write(*,fmt='(\A1)')'|'
  if ( i-(i/3)*3.eq.0 ) write(*,fmt='(\A1)')' '
41 continue
write(*,*)
write(*,*)'-----------------------------------------'

pause 'Press ENTER to close'

End PROGRAM primer

!*****************************************************************
!*****************************************************************

subroutine FINDRF(vector,logicalsize,size,pos,rf)

INTEGER logicalsize,size,pos,rf
INTEGER i,j,s
CHARACTER vector*(logicalsize)
```


Reproduced with permission of the copyright owner. Further reproduction prohibited without permission.

```
s=0
do 10 i=1,pos
  if ( vector(i:i).eq.' ' ) s=i
10 continue
rf=pos-s

end subroutine FINDRF

subroutine FINDENZ(vector,logicalsize,size,string,logicaldim,dim,pos)

INTEGER logicalsize,size,logicaldim,dim,cut,rf,pos
INTEGER i,j,k,match,space
CHARACTER vector*(logicalsize),string*(logicaldim)

do 10 i=1,size
  match=0
  j=1
  k=0
  100 continue
  if ( vector(i+k:i+k).eq.string(j:j) ) then
    match=match+1
    if ( match.eq.dim ) then
      pos=i
    endif
    if ( vector(i+k+1:i+k+1).ne.' ' ) then
      k=k+1
    else
      k=k+2
    endif
    if ( string(j+1:j+1).ne.' ' ) then
      j=j+1
    else
      j=j+2
      match=match+1
    endif
    goto 100
  endif
10 continue

end subroutine FINDENZ

subroutine COUNTNUCS(array,logicalsize,size,nc,ng,nt,na,ns)

INTEGER i,logicalsize,size,nc,ng,nt,na,ns
CHARACTER array*(logicalsize)

nc=0; ng=0; nt=0; na=0; ns=0;
do 10 i=1,size
  if (array(i:i).eq.'C')nc=nc+1
  if (array(i:i).eq.'G')ng=ng+1
  if (array(i:i).eq.'T')nt=nt+1
  if (array(i:i).eq.'A')na=na+1
  if (array(i:i).eq.' ')ns=ns+1
10 continue

end subroutine COUNTNUCS

subroutine BLANK(rdarray)

INTEGER i,amax
PARAMETER (amax=2500)
CHARACTER rdarray*(amax)
```


Reproduced with permission of the copyright owner. Further reproduction prohibited without permission.

```
do 10 i=1,amax
  rdarray(i:i)=' '
10 continue

end subroutine BLANK

subroutine COMPLIMENT(for,size,rev)

INTEGER i,j,k,size
CHARACTER for*(size),rev*(size)
LOGICAL first

do 10 i=1,size
  if ( for(i:i).eq.'C' ) rev(i:i)='G'
  if ( for(i:i).eq.'G' ) rev(i:i)='C'
  if ( for(i:i).eq.'T' ) rev(i:i)='A'
  if ( for(i:i).eq.'A' ) rev(i:i)='T'
  if ( for(i:i).eq.' ' ) rev(i:i)=' '
10 continue


end subroutine COMPLIMENT

subroutine ASSIGN(rdarray,size,array)

INTEGER i,amax,size
PARAMETER (amax=2500)
CHARACTER rdarray*(amax), array*(size)

do 10 i=1,size
  array(i:i)=rdarray(i:i)
10 continue

end subroutine ASSIGN

subroutine REVASSIGN(rdarray,nrd,size,array)

INTEGER i,amax,size,nrd
PARAMETER (amax=2500)
CHARACTER rdarray*(amax), array*(size)

do 10 i=1,size

  array(i:i)=rdarray(nrd-i+1:nrd-i+1)
10 continue

end subroutine REVASSIGN

subroutine CHECKARRAY(array,size)

INTEGER i,size
CHARACTER array*(size)

do 10 i=1,size
  if ( array(i:i).ne.' ' .AND. array(i:i).ne.'C' .AND. &
       array(i:i).ne.'G' .AND. array(i:i).ne.'T' .AND. &
       array(i:i).ne.'A' ) then
    write(*,*)i,array(i:i),' Unknown nucleotide detected.'
    stop;
  endif
10 continue

end subroutine CHECKARRAY
```


Reproduced with permission of the copyright owner. Further reproduction prohibited without permission.

```
subroutine CAPITALIZE(array,size)

INTEGER i,size
CHARACTER array*(size)

do 10 i=1,size
 if ( array(i:i).eq.'c') array(i:i)='C'
 if ( array(i:i).eq.'g') array(i:i)='G'
 if ( array(i:i).eq.'t') array(i:i)='T'
 if ( array(i:i).eq.'a') array(i:i)='A'
 if ( array(i:i).eq.' ') array(i:i)=' '
10 continue

end subroutine CAPITALIZE

!****************************************************************
!****************************************************************

function TEMP(nc,ng,nt,na)

INTEGER nc,ng,nt,na
REAL t

t=4.0*(nc+ng)+2.0*(nt+na)
TEMP=t

return
end function TEMP

function FINDSIZE(array,logicalsize)

INTEGER i,j,k,logicalsize,size
CHARACTER array*(logicalsize)
LOGICAL first,last

first=.false.
last=.false.
size=0
do 10 i=1,logicalsize
  if ( array(i:i).ne.' ') first=.true.
  if ( array(i:i).eq.' ' .AND. array(i+1:i+1).eq.' ') last=.true.
  if ( .NOT. last .AND. first) then
    if ( array(i:i).eq.'C') size=size+1
    if ( array(i:i).eq.'G') size=size+1
    if ( array(i:i).eq.'T') size=size+1
    if ( array(i:i).eq.'A') size=size+1
    if ( array(i:i).eq.' ') size=size+1
  endif
10 continue

FINDSIZE=size

return
end function FINDSIZE
```


Reproduced with permission of the copyright owner. Further reproduction prohibited without permission.

Vita Auctoris

DANA SESLIJA

Education:

1999-2003 B.Sc. Honours Biology, University of Windsor.

2003 - present M.Sc. candidate Biochemistry, University of Windsor.

Publication:

Raturi, A., Vacratsis, O., Seslija, D., Lee, L., and Mutus, M. (2005). A direct, continuous, sensitive assay for protein disulfide isomerase based on fluorescence self-quenching. *Biochemical Journal.* Accepted June 17 as Epub doi:10.1042/BJ20050770.

Reproduced with permission of the copyright owner. Further reproduction prohibited without permission.